

## **General Disclaimer**

### **One or more of the Following Statements may affect this Document**

- This document has been reproduced from the best copy furnished by the organizational source. It is being released in the interest of making available as much information as possible.
- This document may contain data, which exceeds the sheet parameters. It was furnished in this condition by the organizational source and is the best copy available.
- This document may contain tone-on-tone or color graphs, charts and/or pictures, which have been reproduced in black and white.
- This document is paginated as submitted by the original source.
- Portions of this document are not fully legible due to the historical nature of some of the material. However, it is the best reproduction available from the original submission.

(NASA-CR-174380) METAL VAPOR ARC SWITCH  
ELECTROMAGNETIC ACCELERATOR TECHNOLOGY  
Report, 3 Sep. 1983 - 2 Sep. 1984  
(Massachusetts Inst. of Tech.) 60 P  
HC A04/MF A01

N85-18259

Unclas  
14166

CSCI 09A G3/33

**METAL VAPOR ARC SWITCH  
ELECTROMAGNETIC ACCELERATOR TECHNOLOGY**

**Grant Number NAG3-283**

**September 3, 1983 - September 2, 1984**

**Work supported by:  
NASA-Lewis Research Center  
21000 Brookpark Road  
Cleveland, Ohio 44135**

**Principal Investigator  
Dr. Peter P. Mongeau  
Massachusetts Institute of Technology  
Office of Sponsored Programs  
77 Massachusetts Avenue  
Cambridge, Massachusetts 02139**

## High Current Vacuum Arc Switching

### 1. High Performance Switching

#### A. Introduction to Vacuum Arc Switches

#### B. Applications of Interest

### 2. Vacuum Switch Physics

#### A. Arc Initiation

##### 1. Triggered Vacuum Gap

##### 2. Vacuum Interrupters

#### B. Arc Conduction

##### 1. Material Considerations

- \* vapor pressure
- \* transition temperature
- \* erosion/ablation (refer to known rates and mechanisms and dependence on current density)
- \* lifetime considerations
- \* cathode/anode spot formation (dependence on current density)

##### 2. Inefficiencies - power losses identified

- \* electrodes:
  - I<sup>2</sup>R, conduction, phase change energy, ionization, grey-body radiation
- \* arc:
  - collisions arc resistance, radiation, convection, conduction

##### 3. Arc Modes: Diffuse, Constricted

##### 4. Magnetic Field Effects

- \* stabilization
- \* rotation
- \* magnetic field sources

### C. Interruption

#### 1. Passive Extinction

- \* micro-thermal management
- \* field effects
- \* condensation (location/pattern)
- \* arcing history
- \* interruption time

2. Forced Extinction

- \* field effects
- \* counterpulse techniques (Honig)
- \* mechanical (shutter)
- \* interruption time

3. Summary of Interruption Factors- Voltage Recovery

- \* spot cooldown
- \* asperite formation
- \* frequency effects

3. Practical Engineering

A. Heating

- \* Heat Rejection & Cooling Mechanisms
- \* Duty Cycle - single shot, multishot, and steady state capabilities
- \* Anti-Ablative Measures
  - plated electrodes
  - feedable electrodes
- \* Voltage Drop

B. Electrode Lifetime

C. Device Configuration

- \* Electrode Packing Factor, high surface/ volume ratio
- \* Average Current Density
- \* Device Scaling

D. External Circuit Configurations

- \* Counterpulse
- \* Saturable Core
- \* Interrupters/ Contactors
- \* Hybrid Switches

E. Comparison with Competing Devices

SCRs, GTOs, spark gaps, ignitrons, mechanical breakers

- \* interruption
- \* small size
- \* no maintenance
- \* apparent scalability
- \* minimum voltage drop
- \* lifetime issues

F. Applications

4. Point Design

5. Recommendations and Conclusions

6. Appendix - Experimental Research Results  
- References

## 1. High Performance Switching

Advances in electromagnetic propulsion techniques are approaching the present-day technical limits of energy storage, transmission, and switching devices. The desired operating area of such devices is in the range from 100 volts to 20 kilovolts and from 20 kiloamperes to several megamperes. While single shot make switches of these power levels are routinely available they are of limited utility for a practical electromagnetic launcher system. The ability to open or commutate high power circuits repetitively is especially crucial in accelerator technology because it governs repetition rate, efficient multi-stage operation and ultimate velocity.

The most familiar opening switches are solid state devices. Solid state switches (SCR's, transistors, FET's, GATO SCR's, darlington's, etc.) have been used for applications up to the 2 kilovolt, 20 kiloampere range for a 5 msec pulse. [Mongeau, 1982] The desirable characteristics of these devices include the ability to interrupt or rectify at zero current crossing, high gain electronic triggering and essentially zero wear or moving mechanical parts. Much research is presently underway in the power industry to extend the safe operating areas of solid state switches.

### A. Introduction to Vacuum Arc Switches

A device which is operationally quite similar to the high power SCR is the vacuum switch. Like the SCR the vacuum switch can be readily electronically triggered and more importantly can

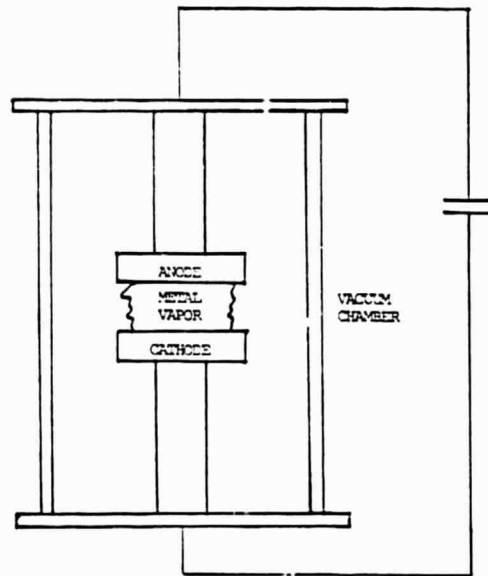


Figure 1-1 Vacuum Switch Schematic

commutate or interrupt at a zero current crossing. A metal vapor vacuum switch is a multi-electrode device housed in an insulated vacuum vessel. Figure 1-1 shows a schematic form of a metal vapor vacuum switch. The conduction medium is an ionized metal vapor generated from the surfaces of the cathode (and possibly the anode depending upon the arcing conditions). Conduction is initiated typically by either separating metal contacts or surface breakdown when a third electrode or trigger electrode applies a high voltage across a dielectric surface. The conduction medium is maintained by power deposition at the electrode surfaces. Conduction continues until some competing particle-loss mechanism overwhelms the particle creation mechanism. Recovery is said to occur if conduction ceases for an indefinitely long period of time. Figure 1-2 shows in block form the phases of the vacuum arc switch.

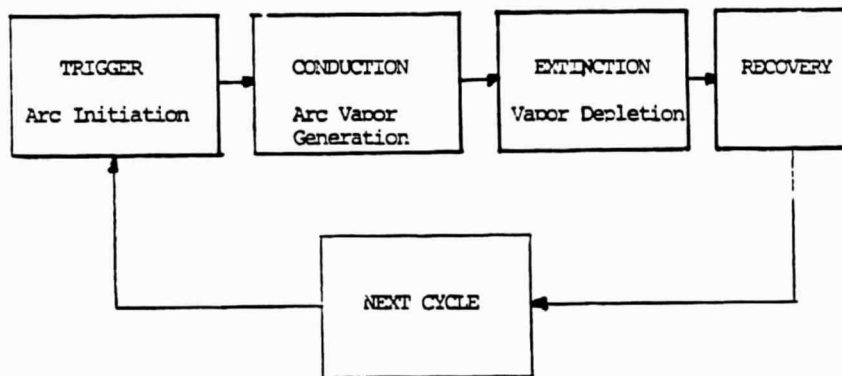


Figure 1-2 Phases of Vacuum Arc Conduction

Both solid state switches and vacuum arc switches are capable of spontaneous interruption at zero current crossing. However, vacuum arc switches are more appropriate for high performance launchers because of their inherently higher power capabilities. Vacuum arc switches have been operated up to the hundred kiloampere level and have held off voltages up to the 100 kilovolt level. SCR's, on the other hand are at present limited to tens of kiloamps and a few kilovolt operation. This several orders of magnitude difference in power level is due to the intrinsic differences in the conduction medium of the two devices. The silicon wafers used in SCR's must be kept fairly thin (less than 1 mm) to keep switching times down and to reduce conduction losses. This requirement limits the standoff voltage to the associated dielectric strength of the thin semiconductor. The peak current capability of an SCR is limited by the ability

of the available thermal inertia absorb ohmic heating. In other words the SCR is current integral limited ( $\int i dt$ ) by a material which has a fairly high resistivity. This often translates to a peak current limit as well governed by how fast the current can increase in a chip in a short enough conduction period. Light activated silicon rectifiers or LASSCR's, for example, have reached 50 kA because of the very high current ramp rates afforded by direct photo-electric injection of charge carriers. In all fairness it should be noted that solid state devices have been designed with very forward voltage drops in mind for efficient operation in low voltage circuits. Recently there has been some interest in using the bulk properties of much thicker semiconductors where very low voltage drops are not important [Nunally]. Metal vapor arc switches, on the other hand, utilize a conduction medium which is a very low density metal plasma with a resistivity that approaches that of stainless steel's. Since the plasma itself has no temperature limits and is regenerated as needed there appears to be no theoretical current limit of a vacuum arc switch. Furthermore, once the switch has recovered the gap has returned to a high vacuum state which is an ideal dielectric capable of holding off very high field gradients. The hard part to be sure is to insure that the vacuum switch does successfully revert to the vacuum state before voltage is applied.

Other gap switches such as gas gap switches and ignitrons are also capable of very high currents and voltages. However, they are not truly commutating switches in that their recovery time is much longer than that of the vacuum gap switch. Vacuum gaps (due to their low density) generally recover voltage standoff in a few microseconds. The de-ionization time of a gas gap switch is generally on the order of a few milliseconds. In an ignitron the gap medium (mercury) must actually recondense which can take tens of milliseconds. The gas gap and ignitron switches can be used in repetitive firing applications but not in applications where the commutation period must be shorter than a millisecond.

There are four distinct phases to metal vapor vacuum arc switching: breakdown, conduction, extinction, and recovery. The initial off-state is maintained by the high dielectric strength of the vacuum. Breakdown of the arc is initiated by high voltage flashover or separating contacts. Arc conduction is maintained by energy deposition at the electrode surface. This energy deposition causes vaporization and subsequent ionization of the electrode material. Commutation depends on the current diminishing to zero, either naturally in an oscillatory discharge or by being forced to zero by counterpulse circuitry. As the current approaches zero, the input power goes to zero. The regeneration rate of plasma then decreases until the generation rate of plasma is less than the total plasma recombination rate. At this point the switch has entered the extinction phase. If the dielectric strength of the gap can reach a sufficiently large value before the voltage is reapplied, then the switch is said to have recovered. Recovery rates for vacuum switches as high as 24 kV/us have been reported [Mitchell, 1970]

At low currents (100-10,000 A for electrodes 5 cm in diameter) vacuum switches are characterized by a multiplicity of cathode spots and an arc voltage of 20-50 V. Cathode spots are highly localized regions of very high current density (10 MA per square centimeter) Each spot is observed to carry a maximum current, which depends on the electrode material (100 A for copper). As the discharge current increases additional cathode spots are formed which carry the current in parallel with the original spots. This explains why the perceived resistance ( less than 5 milliohms) of a vacuum gap switch is so low.

Above some critical current for a given electrode geometry anode spots have been observed [Rich, 1971]. Anode spots are current constriction points on the anode where bulk melting of the electrode metal has occurred. Due to the thermal inertia of an anode spot, which is typically several centimeters in diameter, metal vapor will be emitted into the gap for several milliseconds after a current zero. This prolonged generation of metal vapor prevents the gap from reestablishing a high dielectric strength usually resulting in a failure for the device to commutate. Much of the present research of vacuum arc switches is involved with postponing or eliminating the onset of anode spots.

#### B. Applications of Interest

The objective of this study was to establish the utility of vacuum gap switches in quasi-static high current (megampere level) DC circuits. Railguns, in particular, would benefit greatly from a current that could not only handle the high currents during inductor charging but then commutate the current into the railgun as well. Other accelerators such as multi-stage coaxial launchers could also take great advantage of rapidly commutating high performance switches. Although it is difficult to assess the performance limits of a device which in the last few years has just started to be investigated on a wide level, it is certainly possible to establish the trends and guiding principles which govern the application of vacuum gap switches.

A description of the vacuum switch physics is presented which precedes a discussion of specific engineering issues. Engineering analysis focuses on parameters internal to the switching device as opposed to external to the switch. For example, the average surface current density of the electrodes (internal) is one of the variables controlling the size of the device, while on the other hand, the ultimate performance of the switch depends on whether a capacitive counterpulse or saturable reactor are used in the external circuit.

Electrical schematics are presented which illustrate various applications of vacuum switches. Discharge parameters such as current, voltage, current derivative, and discharge frequency are included in the discussion where appropriate.

A point design is offered for a specific application of current interest. Recommendations and conclusions are offered

which summarize the present advantages and disadvantages of vacuum switches.

## 2. Vacuum Switch Physics

### A. Arc Initiation

There are two different types of vacuum switches: triggered vacuum gaps (TVGs) and separating contacts, also known as vacuum interrupters or contactors.. The main difference between these switches is the method of arc initiation. The arc trigger mechanism, to a large extent, determines the characteristics of the vacuum switch.

Triggered vacuum gaps typically rely on a controlled high voltage surface flashover to inject a small quantity of plasma into the interelectrode region to cause the main gap breakdown. The trigger is a dielectric which has become slightly contaminated with conductive impurities. The trigger current pulse ohmically heats and vaporizes this conductive layer. The layer is regenerated by re-deposition of material during subsequent arc conduction and interruption phases ( there is some training associated with this contaminant layer which can affect trigger reliability). A TVG is useful in applications which have the following requirements: a) normally open switch; b) fast interruption times of order 10 us); c) moderate current-time product ( greater than 1 kA-s); d) repetition rated (of order 1 kHz); e) precise trigger control.

Vacuum interrupters conduct current through electrodes which are normally maintained in contact until interruption is desired. Because of the solid metal to metal contact between electrodes the voltage drop across the interrupter during conduction is extremely low. At the desired time the contacts are suddenly separated. The arc is quite naturally initiated by the initially zero gap breakdown. The time scale for separation is about 3 ms and the separation distance is on the order of 2 cm. Most vacuum contactors are employed by the utility industry where interruption time on the order of a 60 Hz period is satisfactory. Much more rapid contact separation times are undoubtedly possible by resorting to pulse induction techniques [ Sze 1984, ]. A vacuum interrupter is most useful in applications with the following requirements: a) normally closed switch; b) moderate interruption times (of order 1 ms); c) large current-time product (DC operation); d) low repetition rated device (1 interruption cycle per second).

The advantages of TVGs and vacuum interrupters are shown in Table 2-1.

Table 2-1 Advantages of Vacuum Switches

	TVG	Vac. Interr.
good triggering control	*	
fast response	*	
high rep. rate	*	
high voltage standoff	*	*
high current operation		*
electrical-parallel operation	*	*
fast commutation	*	
orientation-independent	*	*
ambipolar conduction	*	*
wide voltage operating range	*	*
normally closed switch		*

B. Arc Conduction

**Material Considerations.**

Electrode performance can be attributed to either surface or bulk effects. A list of electrode material selection criteria in regards to these effects is given in Table 2-2. From a practical point of view material availability, purity, cost, machinability, amount of trapped gases and ease and safety of handling are also important considerations.

Table 2-2 Electrode Material Selection Criteria

Characteristic	Desired aspect
<u>Surface effects</u>	
(1) vapor pressure	low
(2) phase transition temperature	high
(3) erosion rate	low
(4) heat of transformation	high
(5) high voltage standoff	high

Bulk Effects

(6) work function	low
(7) arc stability	(conditional)
(8) electrical conductivity	high
(9) thermal diffusivity	high
(10) mechanical strength	high

**Vapor Pressure**

The vapor pressure is the partial pressure associated with a given material at a specific (uniform) temperature at which the liquid phase and vapor phase are in equilibrium. The importance of electrode material in regard to vapor pressure is easily seen if one considers materials such as zinc. At a temperature of 1000 K, well below typical cathode spot temperature, the vapor pressure of zinc is 0.1 atm. The vacuum arc is in fact burning in a high pressure gaseous ambient atmosphere. The extinguishing capability of a gaseous arc is severely impaired due to the high pressure in the arc. In this case the switch looks more like a gas gap switch than a vacuum gap device. Table 2-3 gives the temperature of various metals at the typical vacuum gap pressure of 1 microtorr.

Table 2-3 Temperatures for Associated Vapor Pressures

<b>Metal</b>	<b>Boiling Point (760 Torr) (K)</b>	<b>Temperature (1 <math>\mu</math>T) (K)</b>
Cd	1040	390
Zn	1185	450
Cu	2840	1120
Fe	3135	1300
Ni	3190	1340
Mo	4880	2080
W	5830	2660

[ (a) O'Hanlon, 1980 ]

### **Transition Temperature**

A high boiling point will have two related effects: i) the vapor pressure will be lower at a given temperature, and ii) rapid cooling due to increased thermal gradients and blackbody radiation. Thermionic emission limits the utility of the refractory metals; in these cases the boiling temperature is too high. A thermal goodness factor  $T_m (k \rho C_p)^{1/2}$  can be derived on the basis of thermal analyses.

### **Ablation Rate**

Electrode erosion is a dominant concern in selecting the appropriate electrode material. Electrode mass-loss of a vacuum switch is directly proportional to the total charge passed through the device. [Rondeel 1975]:

$$M = X Q$$

where  $M$  is the electrode mass loss,  $X$  is the material ablation coefficient, and  $Q$  is the charge passed through the device.

In other words, each atom ablated from the electrode surface generates a characteristic number of electrons which carry the actual discharge current. Table 2-4 shows ablation coefficients and electron emission rates for many metals.

Table 2-4 Cathode Erosion Rates for Vacuum Gaps

<b>Metal</b>	<b>Ablation Rate (<math>\mu\text{g}/\text{C}</math>)</b>	<b>Volume Loss (<math>\mu\text{cc}/\text{C}</math>)</b>	<b>Electrons/Atom</b>
Cd	650	76	1.3
Zn	215	30	3.2
Mg	35	20	7.2
Ag	150	14	7.5
Al	120	44	2.3
Cu	115	13	5.2
Cr	40	5.6	14
Ni	80	11	6.9
Fe	73	8	7.2
Ti	52	11.6	9.6
C	16	7.6	7.0
Mo	47	4.6	21
W	62	3.2	31

[Kimblin, 1973; Plyutto, Ryzkhov & Kapin, 1965]

It should be pointed out that the figures above represent ideal erosion coefficients. In practice the real mass loss can be quite different due to bulk boiling (due to macroscopic ablation) and mass redeposition (not all the arc ions are really lost from the system).

### **Lifetime Considerations**

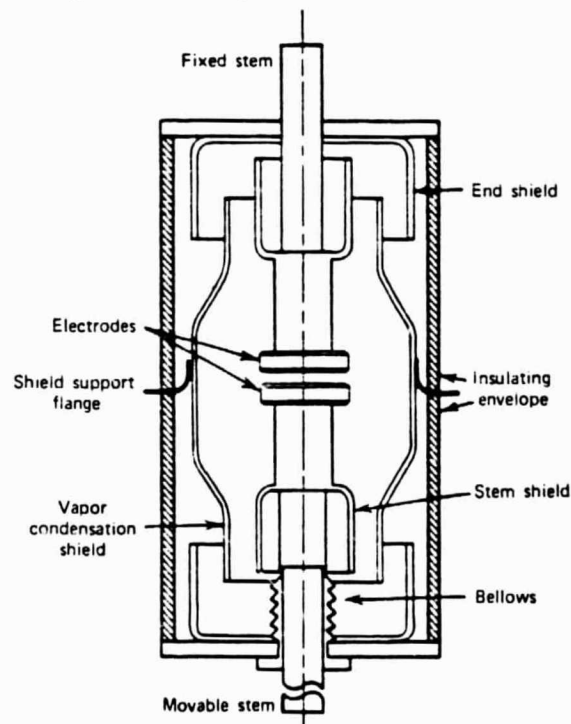
Because of the high vacuum requirements of a vacuum gap switch the vacuum vessel itself is usually constructed of a ceramic cylinder bonded to the metal electrode structures at either end by a permanent solder joint. Such construction prohibits switch service. Some experimental devices, however, are capable of being serviced [Cope, et. al 1983].

Switch lifetime is limited by three processes. First, the vacuum of the device gradually deteriorates as the interior

switch materials continually outgas. The selection of properly refined electrode metals (vacuum remelted, for example) limits this to very low levels. Furthermore, it is standard practice to condition the vacuum chamber by applying a high AC voltage across the electrodes.

The second limiting process is simply the loss of electrode material through ablation. Eventually the electrodes will be sufficiently reduced to seriously affect the gap spacing and geometry. Long before the electrodes reach such a sorry state the third and dominant limiting process becomes evident. In the course of electrode erosion, some fraction of the ablated metal will become deposited on the otherwise insulating walls of the vacuum vessel. Eventually, the dielectric strength of the vacuum vessel becomes so adversely affected that the switch can no longer stand off the rated voltage without some spurious internal surface breakdown.

It is standard practice to use some type of condensate shield to protect the critical interior surfaces of the device from metallic build-up. Figure 2-1 shows such a typical shield in a vacuum switch. It must be noted, however, that simple line-of-sight protection of surfaces is not sufficient to prevent metallic condensation on all surfaces of importance. Several investigators [Tuma, et al, and Jenkins] have reported deposition of condensate on vessel walls outside the solid angle of the arc conduction. Even the back side of the cathode was observed to have anode material deposited upon it.



Cross section of a typical vacuum interrupter.

Figure 2-1 Vacuum Switch with Condensate Shields

In contrast to other types of switches, especially gas gap switches and ignitrons, vacuum switches rely upon the electrode material itself for a conduction medium. This creates a fundamentally different electrode lifetime problem compared to more conventional types of switches.

It has been shown that the electrode material loss of a vacuum switch is indeed a thermal phenomenon - adiabatic heating of the cathode spot. [Cope, Ph.D. Thesis] The current density at the cathode has been measured to be greater than 10<sup>6</sup> Amps/cm<sup>2</sup>. It should be noted that the measured current density has historically increased as the methods used to measure it have improved. Cathode spots are characterized by the spot current and radius depending on the cathode material (see Table 2-5). The very high heat flux associated with the cathode spot actually ablates the cathode surface at a measured rate which is in good agreement with theoretical calculations for a wide variety of metals. [Cope, 1983]

Table 2-5 Cathode Spot Currents and Radii

<u>Metal</u>	<u>SpotCurrent(a)</u>	<u>Spot Radius(b)</u>
Copper	100 A	20 $\mu$ m
Nickel	100 A	5 $\mu$ m
Tungsten	300 A	15 $\mu$ m

(a) Kimblin, 1973; (b) Cope, 1983

In essence, a highly localized thermal equilibrium is established in the first few microseconds of the arc discharge. During the remainder of the discharge the incident electrical power is consumed largely in the heat of vaporization and ionization of the cathode material. Spacecraft re-entry into the earth's atmosphere creates a physically similar effect.

The results of measured ablation rates are typically reported in terms of the peak current passed through the device. Comparison among results of different experimenters' results requires that the total available electrode surface area also be given. For currents of less than about 10 kiloamps on electrodes of about 4 inches diameter, it has been observed that only the cathode actively takes part in the discharge through ablation. For these lower currents, the anode merely serves the space charge requirement of electron collection. The measured cathode ablation rate (referred to as the "erosion rate" in the literature) is approximately constant from a few hundred amperes up to ten kiloamperes for the above mentioned electrode sizes (see Table ).

For currents above approximately ten kiloamps, however, the situation drastically changes. [Mitchell, 1970] At this current level, the anode begins to actively take part in the discharge. A relatively large molten mass of electrode metal forms as an anode spot. Gross melting substantially increases the ablation rate by a factor of 20 to 100. Figure 2-2 shows some measured results for copper. Apparently there is some collective arc phenomena that can cause unstable arc constriction on the anode above some critical current. Presumably a single device's current rating can be increased by incorporating multiple electrode structures within the same vacuum vessel..

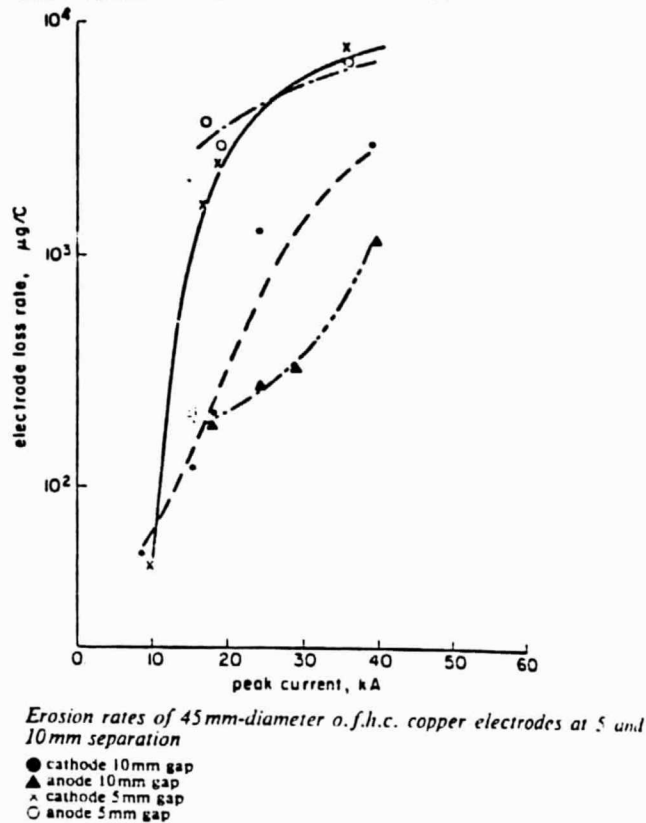


Figure 2-2 Ablation Coefficients Associated with Anode Spots (Mitchell, 1970)

Correlations have been made between material thermal properties and the critical current (that current at which anode spots form.) [Rich, 1971 ?] The thermal "goodness" parameter  $T_B (k \rho C_p)^{1/2}$  has been determined to correlate well with anode spot formation. Table 2-6 shows the thermal goodness parameters and currents at which anode spots formed on electrodes 5.7 cm in diameter for several metals.

Table 2-6 Thermal Parameter vs. Critical Current

<u>Metal</u>	<u>Thermal Parameter</u> $T_m (k\sqrt{\rho C_p})^{1/2}$	<u>Critical Current</u> (kA)
Sn	57	2.3
Al	383	6.8
Ag	723	9.7
Cu	954	10.3
Mo	1204	13.6
W	1693	13.8

The severe penalty for anode formation in terms of material loss has an implication beyond that of simply decreasing the device lifetime. The copious quantities of vapor generated by anode spots and the spots' own substantial thermal inertia greatly increases the voltage recovery time of the switch leading to unreliable commutation. It is important to note, however, that if anode spots have formed previously, there is no a priori reason that the device cannot eventually recover and perform satisfactorily on subsequent discharges.

### **Voltage Drop Losses**

The voltage drop of a vacuum arc switch is a function of the electrode material, electrode spacing, electrode geometry and, to some extent, the total current through the device. As discussed previously vacuum arc switch voltage drop is dominated by the intrinsic arc channel voltage. The electrode material to a large extent determines the arc voltage. Table 2-7 shows some typical voltage drops for vacuum arcs with 2.5 cm opposing plane electrodes.

Table 2-7 Vacuum Arc Voltage Drop

<u>Metal</u>	<u>Voltage Drop</u>	<u>Comments</u>
Cd	11 V	Low B.P., high vapor press.
Cu	20 V	Moderate B.P. and vapor press.
W	25 V	High B.P., Low vapor press.

Physically, the switch power consumption can be attributed to two different sources: the electrodes and the vacuum arc. The electrodes directly interact in a power balance due to ohmic heating of the electrodes, phase change energies, ionization energies (in reality, another phase of the material), atomic potential energies (work function) and grey-body thermal radiation. It is important to note that although in principle only the ohmic heating is non-recoverable energy, very little of the power input to the electrodes is recovered: most is carried away with the ablating particles and deposited at the other electrode or on the vessel walls. These processes can be evaluated as follows:

$$\text{Arc Voltage Drop: } P_{\text{volts}} = VI$$

$$\text{Ohmic heating: } P_{\text{Ohmic}} = I^2 R,$$

$$\text{Phase Change: } P_{\text{phase}} = Hfg \, dM/dt,$$

$$\text{Ionization: } P_{\text{ioniz}} = H_{\text{ioniz}} f \, dM/dt$$

(f = fraction of ablated atoms which are ionized),

$$\text{Work Function: } P_{\phi} = \phi I_e,$$

$$\text{Grey-Body Rad.: } P_{\text{rad}} = \epsilon \sigma T^4, \quad [\epsilon < 1]$$

There are several causes for the arc voltage drop. Power is dissipated by the plasma due to the finite resistance of the arc. Energy is transported by collisions within the arc (primarily electron-electron) through a variety of mechanisms: radiation, convection and conduction. Radiation, however, can be shown to have a negligible effect on the power balance because the plasma is optically thin. The Bremsstrahlung radiation emitted is:

$$\text{Bremsstrahlung: } P_{\text{Brem}} = 1.7E-32 \, n_e^2 \, T_e^{1/2} \, \text{W/cm}^3.$$

$$P_{\text{Brem}} = 3.4 \, \text{W/cm}^3.$$

The convection and conduction terms are quite important. The current streamlines coalesce at the anode immediately before anode spot formation. This indicates that the energy deposited by convection and conduction on the electrode surface is greater than the energy which is carried away by internal anode conduction. The convection and conduction energy transport terms

are evaluated below:

$$\text{Convection: } P_{\text{conv}} = 1/2 \text{ } \rho v^3 A_{\text{arc}},$$

$$\text{Conduction: } P_{\text{cond}} = K_{\text{cond}} (\text{grad } T) A_{\text{arc}},$$

where,  $A_{\text{arc}}$  is the arc cross-sectional area, and  $K_{\text{cond}}$  is the electron thermal conductivity:

$$K_{\text{cond}} = 1.3 \text{ W/cm K.}$$

### 3. Arc Modes: Diffuse and Constricted

Vacuum arcs have been observed to assume different forms during the discharge. [Heberlein 1980] These forms have been correlated with several factors, including the discharge frequency, the electrode geometry, the electrode material and the instantaneous current.

High speed photographic means have enabled researchers to quantify arc forms and to correlate these forms with the arc voltage. Figure 2-3 shows the evolution of the arc mode as the discharge progresses.

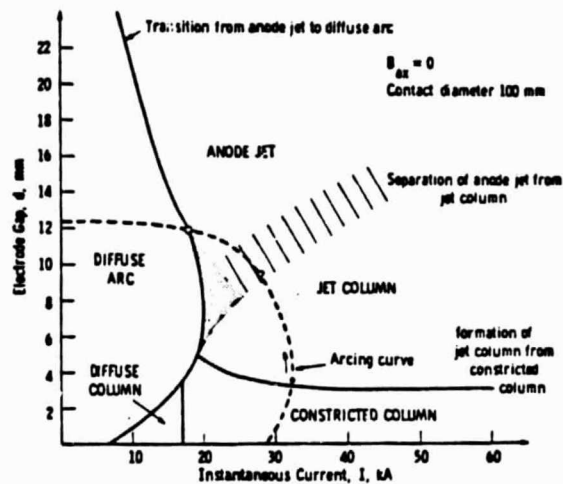


Fig. 7. Physical arc appearance as a function of current and electrode gap, for one half-cycle of arcing, 50-60 Hz, electrode diameter 100 mm,  $I_{sep} > 7$  kA.

Figure 2-3 Arc Modes  
(Heberlein 1980)

To achieve reliable current commutation it is essential to maintain the diffuse arc mode while preventing a constricted discharge from developing. A constricted discharge enhances localized electrode heating and can cause gross melting of sizable areas of the anode (anode spots). The formation of macroscopic melting of the electrodes has a two-fold effect on the interruption capabilities of a vacuum switch. The molten areas are a constant source of particles throughout a current zero crossing, thus competing with the natural depletion rate of the vacuum. In addition the increased erosion rate associated with an electrode melting greatly increases the interelectrode particle density during conduction. This implies a longer plasma dispersion time for the gap dielectric strength to recover.

### 4. Magnetic Field Effects

Magnetic field effects on vacuum arcs have been observed to

be quite pronounced. Magnetic fields have been used as a means to control the arc appearance and arc stability and as a means to move or dislocate the arc path. [Heberlein, Cope, ]

Maintaining an arc in the diffuse mode is important to evenly distributed heating to the electrode surface - especially the anode surface. Prevention of anode spot formation is considered necessary, but not sufficient, to obtain current interruption of the vacuum switch. Magnetic fields parallel to the current path tend to maintain the arc in a diffuse mode. This technique of field utilization will postpone anode spot formation to higher total currents and hence will allow higher currents to be commutated.

The constricted arc mode is the result of a plasma instability. Plasma instabilities have been intensely studied and several of the most common and most destructive instabilities can be readily controlled by the use of magnetic fields.

An alternative method of controlling arc stability is to use the magnetic field to maintain the arc along a desired path. This path may be convoluted so that when the field is brought to zero the arc discharge extinction rate is improved thereby aiding current commutation.

Magnetic blowout is an active technique which is commonly used to deform the arc to a preferred path. By laterally pushing the arc into an elongated or convoluted channel or possibly along a dielectric surface the dielectric recovery rate of the gap can be increased. This approach, it should be noted, is not unique to vacuum switches and has been described in the gas gap literature [Cobine, 1947].

Another magnetic technique is to directly affect the plasma's recombination rate. Because the plasma density in a vacuum switch is so low (as compared to the gas gap plasma) the rate of recombination by collision in the gap is very small. The vacuum gap plasma is generally extinguished by direct dispersion in the surrounding vacuum. By applying a magnetic field to the gap region the cyclotron radius can be decreased to the extent that the chances of an ionizing collision occurring before the particle leaves the gap are large [Hughes ]. Normal conduction is thereby enabled. By bringing the external field to zero, the mean free path for ionization becomes much longer than the electron mean free path. Few ionized particles, hence, become available with which to maintain the discharge. When synchronized with a current zero, this technique is an effective method for improving the recovery of the vacuum dielectric strength.

### **Arc Rotation**

The Lorentz force can be effectively used to circulate the arc over the electrode surfaces even if a constricted arc has formed. By physically forcing the arc power input to the electrode surface to be distributed evenly the formation of large

scale pools of electrode melting associated with anode spots can be effectively postponed. This technique is commonly used in vacuum interrupters as shown in Figure 2-4.

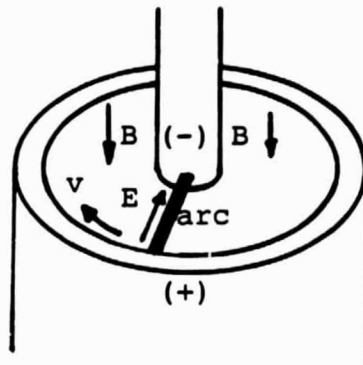


Figure 2-4 Geometry for Arc Rotation

A radial discharge current passing through an axial magnetic field gives rise to a Lorentz force which moves the arc in the azimuthal direction. This action forces the energy input to become distributed along the entire perimeter of the electrodes.

Charged particles gyrate about a guiding center in a magnetic field. The combination of electric and magnetic fields of the arc discharge causes a drift of the plasma guiding centers. Both ions and electrons drift at the same rate independent of the mass or charge state.

The electric field in the rotating frame of the arc is the sum of the (assumed static) radial electric field and the apparent electric field caused by the motion of the arc in the direction perpendicular to the magnetic field. The latter field is similar to the back emf of rotating motors. (Collisions are neglected in this simplified analysis.)

The electric field,  $\underline{E}'$ , in the arc frame of reference is:

$$\underline{E}' = \underline{E} + \underline{v} \times \underline{B}$$

where,  $\underline{E}$  = applied electric field,

$\underline{v}$  = rotational velocity in ( $\Theta$ ) direction,

$\underline{B}$  is the magnetic field.

The net force,  $\underline{F}$ , on the arc constituents is:

$$\underline{F} = nq (\underline{E} + \underline{v} \times \underline{B}) = nq \underline{E}'.$$

where  $q$  = the charge of the plasma particles.

The force on the particles vanishes when the electric field in the rotating frame vanishes, that is, when the rotational velocity is:

$$\underline{v} = \underline{E} \times \underline{B} / B^2 = \underline{E} / B.$$

Hence, the rotational speed is proportional to the electrode voltage and inversely proportional to the perpendicular magnetic field. This form is valid for velocities up to the speed of light. (The electromagnetic field transformation laws could have been used to derive the above equation.)

The use of the guiding center concept in this analysis is valid when the gyro-radii is less than the dimensions of the vessel. The gyro-radius may be written:

$$r_c = mv / eB.$$

This equation implies a lower limit of the  $B$  field when the gyro-radius is comparable to the dimensions of the gap.

Thermal analyses based on this rotational speed have been performed to determine the most desirable speed for a given geometrical arrangement. Overheating a localized spot must be minimized while maximizing the length of time until the spot completes one entire circulation so that cooling mechanisms can prepare the spot for the next cycle.

A steep thermal gradient within the electrode material

proves to have a dominating influence on the temporal development of the spot. Longer arc dwell times tend to reduce this gradient. Therefore maximum effect from the rotating arc is obtained at the rotational speeds which yield the maximum temperature gradient.

Surface non-uniformities, especially asperite formation, will cause the arc to jump or skip between sites. The increased electric field near these sites indicates an increased equilibrium rotational velocity. To take maximum advantage of the electrode thermal inertia, a comparatively rapid rotation rate is appropriate for heavily marred surfaces.

**Magnetic Field Sources**

The concepts described above are valid independent of the source of the magnetic field. However, some of the techniques such as arc rotation can take best advantage of the field created by the discharge current itself. In other cases like the magnetic blowout an external field source is required to interact with the plasma when the discharge current is zero.

There are geometrical configurations which have been designed with the above described concepts in mind. In the case of arc rotation it is desirable to generate self magnetic fields such that the field is parallel to the vacuum arc discharge current. From the Biot- Savart law

$$B = \frac{\mu_0}{4\pi} \int \frac{d\vec{l} \times \hat{r}}{r^2}$$

it can be seen that to do this the discharge current must change vector directions with respect to the gap current vector somewhere within the device. Table 2-8 lists the vector combination which allow for fields parallel to the discharge current, while Figure 2-5 shows the schematic representation of these geometries.

Table 2-8 Geometries Featuring Parallel I and B

<u>Geometry</u>	<u>I</u>	<u>B</u>	<u>Lorentz Arc Motion</u>
Rod Array	z --> $\theta$	$\theta$	no
Spiral Cut	$\theta$ --> z	z	yes
Pie-Spoke (fluted)	r --> $\theta$	$\theta$	no
Wrapped Cylinder	$\theta$ --> r	r	yes

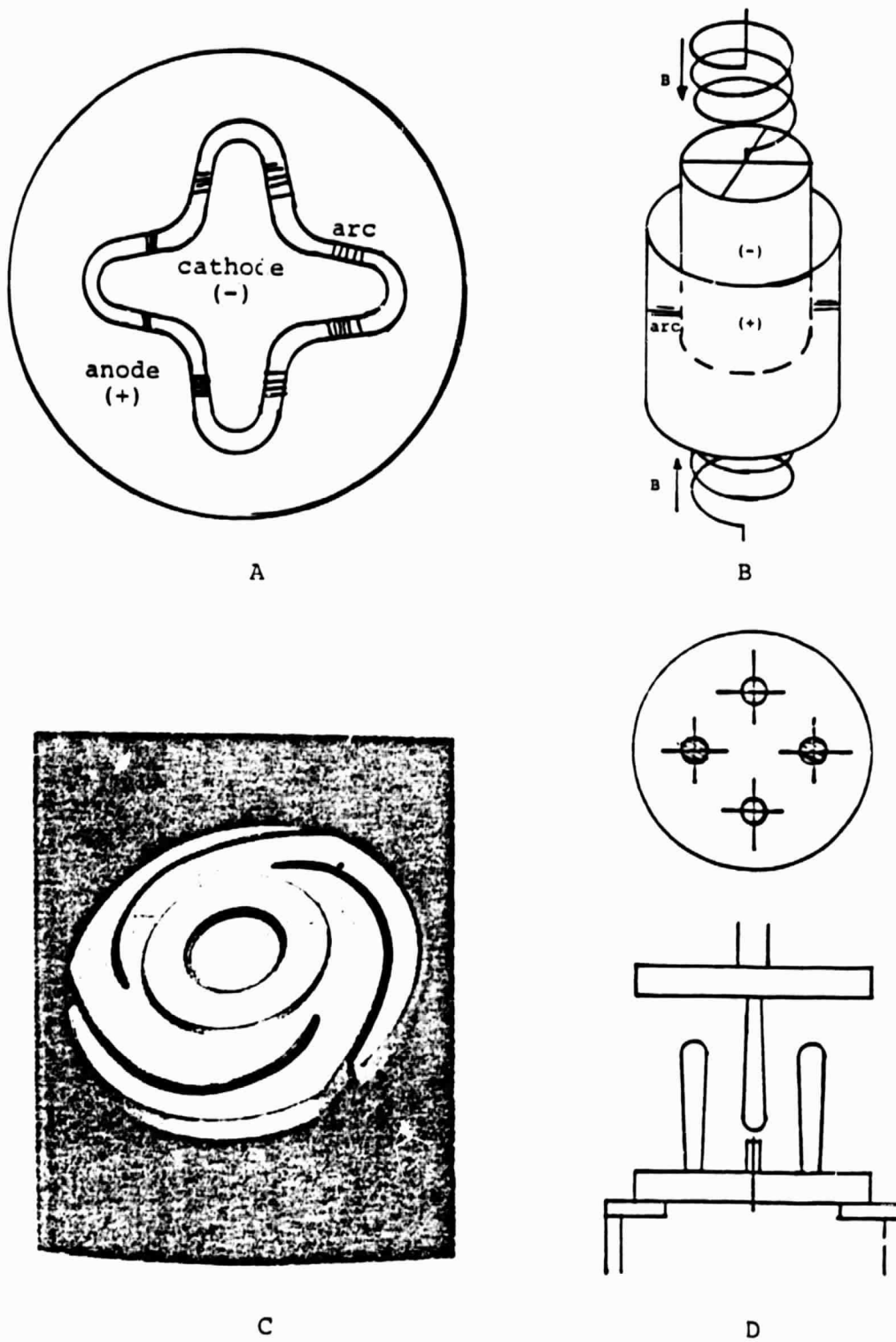


Figure 2-5 Parallel Self Field Configurations

## C. INTERRUPTION

### 1. Passive Extinction

A vacuum switch will spontaneously commutate when the current is held to a sufficiently low value for a sufficiently long period of time. The dielectric strength of the vacuum environment may recover in as little as a few microseconds following the current commutation. This phenomenon will be referred to as passive or self extinction. It is in contrast to forced extinction which is the subject of subsequent paragraphs. The ability of vacuum switches to interrupt current of reasonable magnitude very quickly and to withstand high voltage makes them of practical interest.

A major issue in the study and use of vacuum switches is the investigation of the mechanisms which aid or impede arc interruption. A description of the most important of these mechanisms follows.

Although the vacuum arc is in a constant state of flux, it has been shown [Lafferty, Kimblin] that the vacuum arc is able to respond very rapidly to changes in exterior electrical parameters such as voltage and current. The typical time scale of arc response is a few microseconds.

The effect of this dynamic re-establishment of equilibrium is the absence of "memory" in the plasma: to a very good approximation, a vacuum arc can be described by its instantaneous parameters without any hysteresis effects. Furthermore, it is reasonable to assume that the arc is in instantaneous equilibrium throughout the discharge.

The vacuum arc plasma is characterized by a mean free path which exceeds the arc dimensions. The plasma is thereby governed not by ordinary diffusion equations, but by free-flight equations. Time of flight calculations agree with the observed arc time scale of a few microseconds. Because the Debye length is very small compared to a typical plasma dimension the response of the plasma is limited by the slower ions. Table 2-9 shows a simple free-flight calculation for the ions. Because of the rapid dispersion time of the ions a vacuum arc can be supported only by the continuous injection of ions or neutrals into the gap region.

Table 2-9 Free-flight Calculations

$$\text{Debye Length} = 5 \times 10^{-5} \text{ cm}$$

$$\text{plasma dimension} = d = 1 \text{ cm}$$

$$v_{\text{thermal}} = 10^6 \text{ cm/s}$$

$$t_{\text{free flight}} = d / v = 1 \mu\text{s}$$

The vacuum plasma density is instantaneously proportional to the discharge current [Boxman]. A very simple-minded theory of balancing rates can be used to explain this relationship. In essence the plasma generation rate from the electrodes is self stabilizing with respect to the plasma loss rate to the surrounding vacuum. If the plasma loss rate is at any point in time higher than the plasma generation rate then the plasma density in the gap will start to decrease. As this happens the effective channel resistance and gap voltage will start to increase. The associated rise in power being delivered to the electrodes will cause an increase in the plasma generation rate thus restoring equilibrium to the plasma density. If the current delivered to the switch is increased the increased plasma generation rate must be balanced by an increase in the loss rate as well. This can only be accomplished by an according increase in the plasma density in the gap (the plasma loss rate is strictly proportional to the gap plasma density).

Similarly, the extinction process may be viewed as a competition between particle-creation and particle-loss mechanisms. As the current approaches zero the input power and plasma generation rate also vanish (with the possible exception of hot anode spots). The normal particle-loss processes then have no competition and the gap plasma density will exponentially decay to zero. Naturally, arc commutation can be achieved more readily by increasing the particle-loss mechanisms. According to the above theory enhanced loss mechanisms would imply a higher voltage drop during the conduction phase unless these losses could be selectively applied only during the interruption phase.

Several of these techniques employed to aid gas gap interruption are appropriate to vacuum arc interruption as well. One obvious approach is to increase the particle loss rate by increasing the arc surface area. The flux of plasma due to random motions can be written as:

$$F = nv/4.$$

The units of  $F$  are particles per unit surface area per unit time interval. The surface area of the arc may be increased by simply lengthening the interelectrode gap. Separating contact vacuum interrupters rely on this mechanism. Unfortunately, mechanical motion of the contacts requires a relatively long time (several milliseconds).

A more rapid arc lengthening can be created by the technique of magnetic blow-out. A magnetic field of sufficient magnitude will cause the arc to deviate (blow out) from the established conduction path. This deviation will lengthen the arc, thereby increasing the surface area through which plasma particles may exit.

The arc voltage may be written as a sum of voltage drops corresponding to the choice of electrode material,  $V_0$ , and arc length,  $s$   $dV/dx$ :

$$V = V_0 + s \, dV/dx.$$

Lafferty has studied the effects of post interruption voltage imposed across a vacuum gap as a function of the elapsed time after current zero. [Lafferty, 1966] He found that the applied voltage necessary to re-ignite an arc following a current pulse rose steeply immediately after current zero, but then approached a constant value for times long after the pulse. The rapidly rising breakdown voltage was evidence of the vacuum gap recovering its dielectric strength as the ionized particles left the interelectrode volume. The constant value of voltage required to break down the gap was indicative of the DC dielectric strength of the gap. The measured time scale for voltage recovery was approximately 2  $\mu$ s.

The influence of the electrodes upon interruption must also be considered in any design of a vacuum switch. As mentioned in Section 3, cathode spots are formed which represent very localized areas of intense heating. The temperature of the cathode spot is roughly the boiling point of the cathode material. Hence, there are small molten areas on the cathode surface. It can be shown by a micro-thermal energy management analysis that these areas are in equilibrium with a time constant for cooling only slightly longer than the vacuum arc. [Cope, 1983] In addition, observations show a rapid time dependence of emitted radiation of spots. [Grissolm & Newton 1974]

The temperature of the cathode spot varies with the electrode material. Refractory materials such as tungsten and molybdenum have very high boiling points. These materials have a cathode spot temperature which is sufficiently high that Fowler-Nordheim field emission may contribute to breakdown and re-ignition of the interelectrode plasma, especially if metal splatter causes the formation of asperites. Asperite formation is common for molten surfaces subject to a high electric field gradient. At the other end of the spectrum low boiling point metals such as cadmium or zinc have such low boiling temperatures that vaporization of these metals occurs quite easily and the metals cannot be cooled with sufficient rapidity to stop the evolution of vapor.

Another material phenomenon is that of "current chopping." Current chopping occurs for a particular metal when the drawn current is less than that required for steady state energy balance. [Cope, Thesis] The current will fall abruptly to zero from a value characteristic of the electrode material but typically of several amperes. [Lafferty, 1966] This sudden current reduction may cause a hazardous situation by inducing

excessive voltage rises around the exterior circuit.

Figure 2-6 shows the average arc lifetime for several metals versus the arc current. As shown in Figure 2-7, when the arc lifetime becomes less than the time remaining in the current half-cycle, the arc abruptly extinguishes.

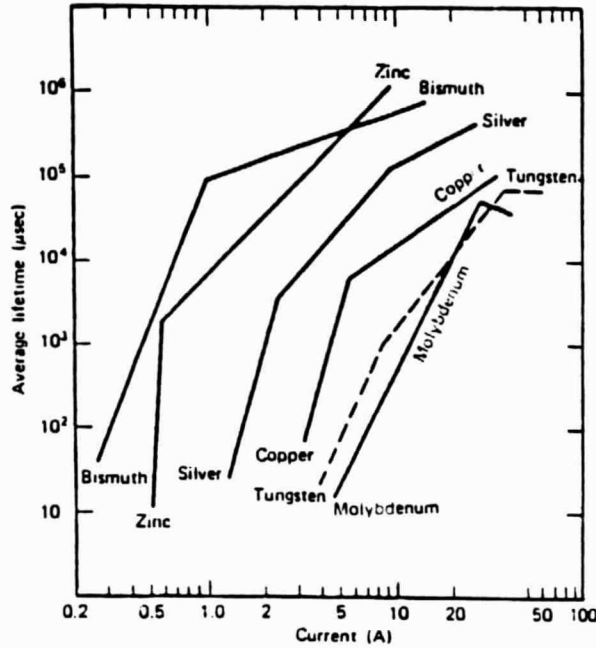


Figure 2-6 Average Arc Lifetime vs. Arc Current (Farrall, 1980)

ARC LIFETIME SIGNIFICANCE

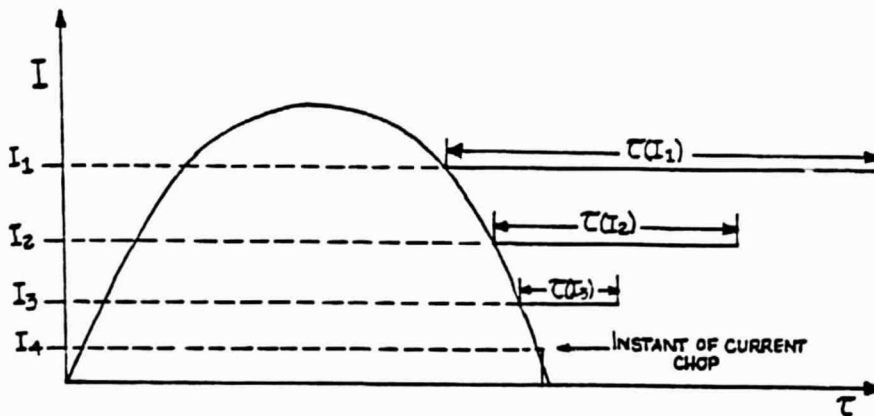


Figure 2-7 Graphical Explanation of Current Chopping

In a vacuum environment, particle loss rate can be increased by enhancing recombination. By providing surfaces upon which the plasma may recombine. A baffle arrangement may be used to effect this technique.

A hybrid approach to arc interruption features the magnetic field propelling the arc onto surfaces for recombination. This approach is similar to that used in arc chutes for gas gaps. In the gas gap case, forced gas flow or the self magnetic field provides the force for pushing the arc into the chute structure.

Section 2, on vacuum switch conduction, discussed the need to shield critical high voltage standoff components from the condensate flux. The particle flux incident upon a wall surface is not totally absorbed - a certain fraction of the flux is reflected ( a "sticking" coefficient of about 0.5 has been measured). A small vacuum vessel volume can cause the reflected particles to rebound near to the electrode gap soon after the particles vacate the gap. A larger vacuum vessel, on the other hand, will prevent re-introduction of the particles into the gap.

## 2. Forced Extinction

There are several techniques available by which one may force the discharge current to zero other than by waiting for a naturally occurring current zero. Current counterpulse and saturable inductor methods are well known [ Honig, 1983, 1984 ] Mechanical shutter techniques, while workable in principle, have yet to be implemented practically. These techniques basically attempt to produce a near zero gap current for a time long enough for the switch to establish a high dielectric strength state.

There is another technique which more directly attempts to clear the gap of charge carriers. A magnetic field at an angle to a current carrying element exerts a force on that element. This is the Lorentz force, also known as the "J cross B" force. The force per unit conductor volume is f:

$$\vec{f} = \vec{J} \times \vec{B}.$$

or per unit conductor length:

$$\vec{dF} = I \vec{dl} \times \vec{B}$$

The Lorentz force acts directly on the current element, in this case, the vacuum arc charge carriers. The field, of course, is most efficiently used when it is at right angles to the current and the resulting vector cross product is along the desired direction of motion.

There are several geometrical configurations suitable for such an application. An opposing planar geometry has historically

been the most common arrangement. The field is simply applied in a direction transverse to the gap. Figure 2-8 shows a cross-section of a planar gap with a magnetic field applied perpendicular to the paper. Note that the return path for the magnetic flux is not shown.

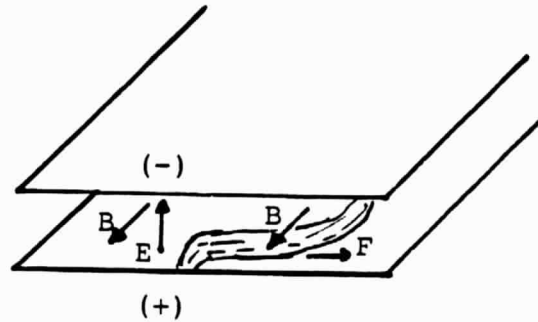


Figure 2-8 Planar Current-Field Interaction

Coaxial geometries offer significant advantages over rectilinear ones because of simplified device construction and the ability to establish a local flux return path. In this case either passive or active magnetic fields can be used. Figure 2-9 shows four different coaxial arrangements. We have performed experimental investigations of the geometries in Figure 9- A and D. These two topologies appeared to be the best from the standpoint of simplicity, construction techniques, theoretical considerations (such as anode spot avoidance) and previous experience with similiar geometries.

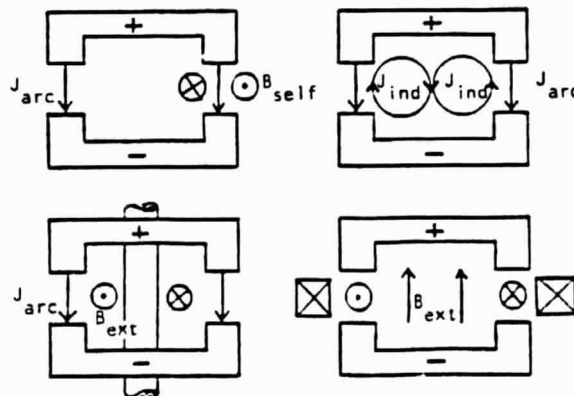


Figure 2-9 Coaxial Magnetic Field Configurations

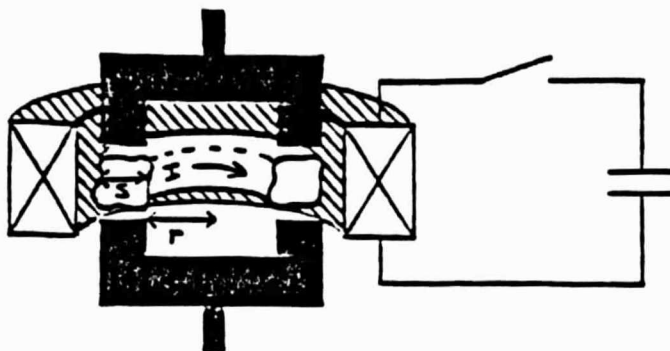


Figure 2-9A Ideal Coaxial Augmented Field Geometry

A simplified analysis of the interaction of the conducting plasma and the pulsed magnetic field indicates that plasma expulsion can be achieved within 10 us under typical pulsed conditions. For example, consider the idealized configuration shown in figure 2-9A. In this analysis the plasma can be thought of as the secondary in a pulse transformer while the external pulse coil is the transformer primary. The voltage induced in the secondary is:

$$V = \frac{d\Phi}{dt} = \pi r^2 \frac{dB}{dt}$$

where  $r$  is the radius of the plasma. Assuming a sinusoidal excitation frequency ( $\omega = 2\pi f$ ), the complex amplitudes are:

$$V_0 = \pi r^2 \omega B_0$$

This voltage gives rise to an induced current in the secondary:

$$V_0 = I_0 Z$$

where  $Z$  is the complex impedance:

$$Z = [R^2 + (\omega L)^2]^{1/2}$$

and  $R$  and  $L$  are the plasma-torus resistance and inductance, respectively. The radial force density acting on the plasma is:

$$f = f_a = J \times \frac{B}{c} = \frac{IB}{c s^2}$$

Assuming a constant average acceleration equal to one-half the peak acceleration, the distance  $d$  the plasma moves in a time  $t$  is:

$$d = I_0 B_0 \frac{t^2}{4 \rho s^2 c}$$

Combining the above equations, we arrive at the minimum magnetic field amplitude  $B_0$  necessary to displace the arc a distance  $d$  in the specified time  $t$ :

$$B_0 = \frac{2}{t} \left[ \frac{\rho d s^2 c^2 (R^2 + (\omega L)^2)}{\pi r * r * \omega} \right]^{1/2}$$

This minimum field is plotted as a function of excitation frequency with interruption time as a parameter in Figure 2-10. At high frequencies the minimum field reaches an asymptotic limit of:

$$B_0 = \frac{2}{t} \left[ \frac{\rho d s^2 c^2 L}{\pi r * r} \right]^{1/2}$$

These asymptotic fields are of the order of a few kilogauss and are readily generated externally.

**MAGNETIC FIELD REQUIREMENT**

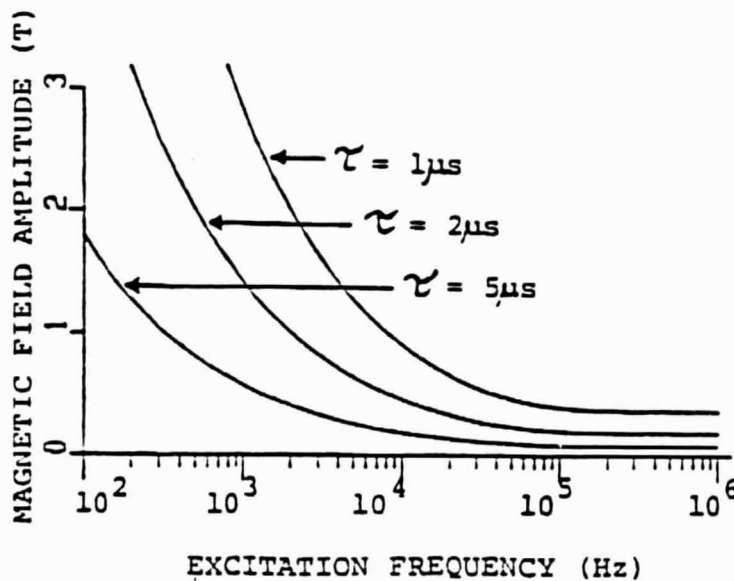


Figure 2-10 Expulsion Magnetic Field Requirement

### 3. Summary of Interruption Factors

The voltage recovery of a vacuum switch is influenced by several factors which are summarized in Table 2-10.

Table 2-10 Factors Influencing Natural Voltage Recovery

<u>Factor</u>	<u>Effect</u>
vapor pressure	high vapor pressure implies copious vapor emission
peak current	increase erosion products; increase plasma density
current duration	thermal expulsion of trapped contaminant gases
$T_m(k\rho C_p)^{1/2}$	increase of erosion products
frequency of current and voltage	allowable escape time decreases with increasing frequency
electrode separation	required escape distance increases, condensation solid angle decreases, neutralizing ion space charge solid angle decreases
gas-free electrodes	vacuum re-melting eliminates trapped gases
thermionic emission	emission through current zero, may provide initial electrons which re-ionize gas
asperite formation	small radii: enhanced Fowler-Nordheim field emission
small atomic mass	increased particle velocity
electrode surface area	anode spot constrictions
parallel magnetic field	retain diffuse arc mode; suppress arc instabilities

[Farrall, 1980; Kamakshaiah and Rau, 1977; Miller and Farrall, 1965; Rich and Farrall, 1973]

All of these effects must be taken into account when designing vacuum switches. In addition experimental results suggest that the product of discharge frequency and current magnitude is approximately a constant for a given switch device (see Appendix for experimental results). This is consistent with the balancing rate theory of arc equilibrium. As the peak current is increased the number of charge carriers which must be cleared from the interelectrode region also increases. Hence a greater time (and smaller frequency) is required for the density to decay to a value which will permit voltage recovery.

### 3. PRACTICAL ENGINEERING

#### A. Heating

Vacuum switch thermal energy management is important in cyclic operation or when a single discharge is long compared to the thermal inertial time period of the switch. The major concern is to limit the peak bulk temperature of the electrodes. Because of the vacuum environment heat rejection is limited to conduction and forced convection through the electrodes themselves and their support structure.

Most vacuum switches in use today are primarily single shot devices where the maximum duty cycle is not well established. The energy deposited per shot can be approximated by

$$dU = I V_s (dt)$$

where  $V_s$  is the switch voltage drop. To be sure some of the energy generated in the current conduction phase escapes via black-body radiation and recombination on the device walls. However, for most applications, the thermal input can be treated as adiabatic where all of the losses eventually are deposited on the electrodes.

Single shot thermal limits can be calculated by a simple linearization of the thermal conduction equation

$$\frac{u}{A} = C_p \Delta T d$$

where  $C_v$  is the specific heat and  $K$  is the thermal conductivity. The thermal diffusion depth into the electrodes is approximately

$$d = 2 \sqrt{\frac{kt}{C_v}}$$

The amount of energy the electrodes (predominantly the cathode) can adiabatically discharge for a given duration is

$$\frac{u}{A} = 2 \Delta T \sqrt{K C_v t}$$

Since the vacuum arc has a fairly constant voltage drop ( approx. 50 volts) we can assign an approximate electrode average current density

$$J = \frac{2 \Delta t}{V_{arc}} \sqrt{\frac{K C_v}{t}}$$

Table 3-1 summarizes the current density and energy flux for two of the more common electrode materials, copper and tungsten.

Table 3-1 Adiabatic Electrode Heat Flux and Current Density

discharge period (sec)	Copper T = 1060 C		Tungsten T = 3360 C	
	heat flux (j/cm )	current density (kA/cm )	heat flux (j/cm )	current density (kA/cm )
1 $\mu$ s	7.7	154	12	240
10 $\mu$ s	24	48	39	76
100 $\mu$ s	77	15	120	24
1 ms	240	4.8	390	7.6
10 ms	770	1.5	1200	2.4
100 ms	2400	0.5	3900	0.8

Rep-rated service would, of course, require some continuous cooling capability. Conduction and forced convection analysis are presented in figure 3-1 for a typical switch. These numbers can be scaled to allow for increased current .

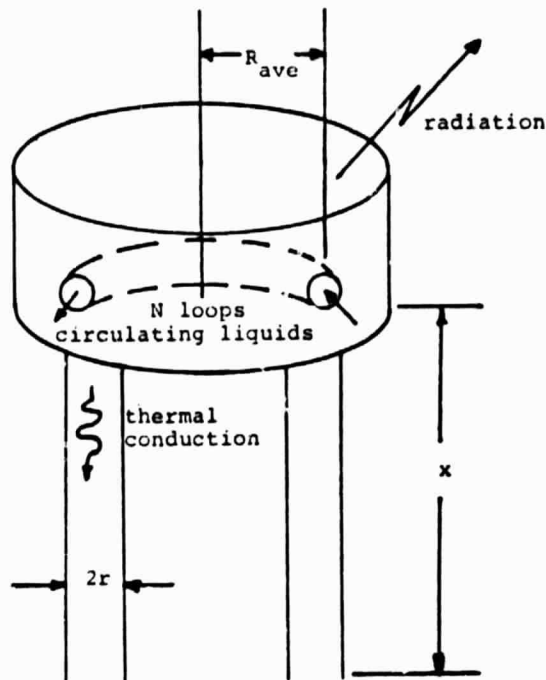


Figure 3-1 Conductive and Convective Switch Cooling Analysis

$$P_{cool} = P_{cond} + P_{conv} + P_{rad}$$

$$P_{cond} = A_{cond} \times K_{thermal} \times \Delta T / \Delta x$$

$$P_{conv} = A_{conv} \times h_{transfer} \times \Delta T$$

$$P_{rad} = A_{rad} \times \sigma_{Stefan-Boltz} \times T^4$$

Assumptions:

Energy Deposited per shot = U

U = 20 kA x 50 V x 100 us = 100 J

$\Delta T = 100$  K (temperature difference for many shots)

$\Delta x = 5$  cm

$$A_{cond} = 2 \times \pi r^2 = 2 \times 1.27 = 2.54 \text{ cm}^2$$

$$A_{conv} = N \times 2\pi Rave d = 2 \times 2 \times 9 \text{ cm} \times 1.27 \text{ cm} = 150 \text{ cm}^2$$

$$A_{rad} = \pi R^2$$

$$h_{transfer} = 100 \text{ BTU/hrft}^2 \text{ F} = 0.057 \text{ W/cm}^2\text{K} \text{ (circulating liquids)}$$

$$K_{thermal} = 4 \text{ W/cm}^2\text{K} \text{ (copper conductor)}$$

Results:

$$P_{cond} = 400 \text{ W}, \quad P_{conv} = 855 \text{ W}, \quad P_{rad} = 12 \text{ W}$$

$$P_{cool} = P_{conv} + P_{cond} + P_{rad} = 1267 \text{ W}$$

Cooling time = the time required to cool an amount of energy equal to one current pulse.

$$\text{Cooling time} = U / P_{cool} = 80 \text{ msec.}$$

$$\text{Duty Cycle} = \frac{\text{Discharge time}}{\text{Cooling time}} = 0.1\%$$

$$\text{Repetition Rating} = 1 / \text{Cooling time} = 12 \text{ Hz}$$

The fact that a vacuum arc has an inherent minimum voltage drop can be a disadvantage in applications where the power supply is operated at a comparatively low voltage. In an HPG/Inductor circuit, for example, the charging voltage from the HPG may only

reach 100 volts. A 50 volt drop in charging voltage represents an unacceptable penalty. A vacuum interrupter, however, can sustain large currents with very low losses. The intrinsic arc voltage only appearing when the electrodes separate. On the other hand the arc voltage is barely noticeable in high voltage applications such as capacitor/pulse coil circuits. Furthermore, the oscillatory discharge provides natural current zeroes for commutation.

### **B. Electrode Lifetime**

Vacuum switch electrodes are exposed to a severe environment. Ablation, neutral particle impact and high temperatures combine to produce a situation where a single metal cannot have all the desirable mechanical, thermal and electrical properties.

The recent acceptance of vacuum switches in the power industry is largely due to the development of high purity vacuum remelted metals. The very low amount of dissolved gases in the electrode material makes it possible to maintain a good vacuum after thousands of discharges.

Perhaps the ideal electrode structure would consist of a high purity copper base ( for high thermal and electrical conductivity) coated with a refractory metal such as tungsten. The composite electrode would offer a higher erosion resistance and lifetime over that of copper alone yet retain the good energy management properties of copper.

### **C. Device Configuration**

Vacuum switches are generally smaller than interrupting gas gap switches of the same current rating. This is primarily due to the small average wall energy-flux and the fact that the vacuum switch interrupts spontaneously. Gas gaps frequently require a flow of a high pressure gas (air) to extinguish the arc.

Because of the importance of preventing gross molten areas on the electrodes, is it desirable to have a rather large electrode surface area available for conduction. A large ratio of the active surface area to the volume of the device is a measure of the space efficiency of the device. Note that this measure is a ratio of area/volume and hence the dimension of this ratio is 1/length. Switches already in use have a ratio of approximately 0.04 /cm. More recently designed devices have ratios in the range of 0.15-0.20 /cm.

The vacuum arc is unique in that it has a positive resistance coefficient; i. e. the arc voltage increases with current. In gaseous arcs the situation is reversed: the arc voltage decreases with increased currents. Using several gas gap switches in parallel is therefore unstable because one of the gaps will tend to dominate. Vacuum arc gaps are quite stable in parallel which makes it possible to operate many gaps closely

together in parallel ( even in the same vacuum enclosure) thus making for a very high packing density. In fact the same phenomenon is evident in a single gap-electrode structure. As the electrode current increases more cathode spots are simply added to handle the greater current requirements.

An electrode structure, which is simply composed of opposing parallel planes, can suffer from electromagnetic attraction of parallel currents at the anode. Essentially, the individual cathode spot currents coalesce into one current channel at the anode. Note that this occurrence would leave most of the anode surface area unused. This sequence of events is likely to lead to the formation of anode spots and so is undesirable.

Electrode structures which separate different parallel anode current paths are advantageous. These structures force the discharge current to maintain distinct current channels and hence they will more evenly distribute the current over the available anode area.

Figure 3-2 shows a schematic of the geometry which was chosen as the baseline for our preliminary experiments (see appendix). Note particularly that this design addresses each of the issues described above. The axial current creates an azimuthal magnetic field. The electrodes are arranged so that the vacuum discharge is actually in the azimuthal direction: thus the field is parallel to the current in the discharge volume. The interdigitated electrode structure of this device provides a large ratio of surface area to enclosed volume. The division of parallel current paths helps to maintain the distinct discharge channels. The anode current thus cannot coalesce into one channel.

A prototype rod array vacuum switch constructed by Rich of General Electric Co. has interrupted 80 kA of power frequency current at a current zero. The material used for the electrodes was carefully selected. The electrodes were of a double vacuum melted material available commercially from Teledyne Vasco. (The advantage of vacuum melted metal is that trapped gases present in metal processed in other atmospheres are thereby eliminated. Trapped gases can become superheated and burst from beneath the electrode surface which introduces additional material into the plasma.) The GE device had an available anode area of  $120 \text{ cm}^2$  and a nominal current density of approximately  $670 \text{ A/cm}^2$ . The space efficiency factor of  $0.04 / \text{cm}$  is rather low for this prototype device, but design optimization should improve that figure by a factor of 2 to 3.

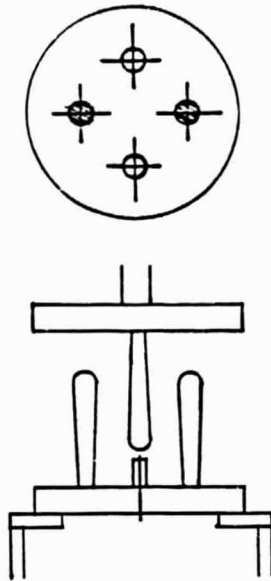


Figure 3-2 Rod Array Design

### Average Current Density

A particular vacuum switch is designed on the basis of the maximum current which is to be interrupted and the standoff voltage required. Comparisons of the operating capabilities of various switches indicate that an average current density of up to 650 A/cm<sup>2</sup> is an appropriate limit for design of vacuum switches.

The value given is only an approximate figure and has been observed to vary by more than a factor of 2 for different materials. A value of 650 A/cm<sup>2</sup> has been experimentally determined for the geometry of rod array electrode structures; the electrodes themselves were fabricated from VascoMax, a vacuum re-melted maraging steel. Values of the average current density as low as 300 A/cm<sup>2</sup> have been observed for small radius, ordinary stainless steel cup electrodes.

### Scaling

By way of example the scaling of the rod array is investigated to determine whether higher current devices are feasible. An important issue is the effect of increased scale size on the device's magnetic fields. The azimuthal magnetic field around an infinitely long conductor may be used as a first order approximation to the actual field. The field is given by:

$$B = I/5R,$$

where,

B is in Gauss, I is the current in amps, and R is the radius of the electrode structure in centimeters.

The maximum current which may flow through the device is limited by the maximum current density which the particular material will support without forming anode spots and the area available for conduction:

$$I = 2\pi N r h J_{\max}$$

where,

r is the electrode radius, h is the vacuum arc height on the electrode, N is the number of cathodes, and  $J_{\max}$  is appropriately chosen for the material.

The electrode structure radius is determined from the geometry of the rod array. It can easily be shown that the radius is related to the electrode radius, r, and the distance between electrodes, s, by the following:

$$R = \frac{r+s}{2 \sin \frac{\pi}{N}}$$

For large N we may approximate R as:

$$R = \frac{N(r+s)}{2\pi}$$

The magnetic field may be written:

$$B = \frac{I}{5R} = \frac{2\pi^2 N r h J_{\max}}{5N(r+s)}$$

Note that the dependence of B on N has cancelled out: more electrodes mean more current can be carried, but the radius must be made larger to accommodate the rods. As the electrode radius is increased the improvement in B is less, so at large r, e.g.  $r \gg s$ , the field magnitude becomes independent of electrode radius. Increasing electrode spacing, s, decreases B due to the larger overall structure radius. Of course, improvements in capabilities of materials, represented by  $J_{\max}$ , increase the magnetic field.

There is a minimum electrode radius which can satisfy the plasma stability criteria. The stability requirement may be written:

$$B_z^2 > 0.5 B_\theta^2$$

alternatively,

$$B_z > B_D / \sqrt{2} .$$

The evaluation of  $B_z$  and  $B_D$  yields:

$$B_z = I/5R = 2 I/[5N(r + s)],$$

and,

$$B_D = I'/5r',$$

where,  $I' = I/N$  and  $r' \cong r$ .

The minimum electrode radius is:

$$r_{min} = \frac{S}{2\pi\sqrt{2}-1}$$

This minimum electrode radius satisfies the plasma magnetohydrodynamic stability requirement. In practice, the requirement is usually easily met. As an example, for  $N = 4$  and  $s = 1$  inch,  $N' = 7$  so  $r > 1/7$  inch.

Another scaling parameter is the scaling of the electrode area per unit volume of vacuum switch. A space efficient switch will have a large ratio of the area to volume.

We assume an array of electrodes arranged on the periphery of an  $N$ -sided polygon. Since two electrodes are needed to complete the circuit, the surface area available for arcing is:

$$A = 2\pi r h N$$

where the definitions are as above.

The minimum vessel volume is:

$$V = \pi r^2 h$$

where  $R$  is the radius of the electrode array.

The ratio  $A/V$  may be evaluated:

$$\frac{A}{V} = \frac{4\pi^2 r}{(r+s)^2 N}$$

$A/V$  decreases proportionally to  $1/N$ . This makes larger devices less space efficient. This is a result of the electrodes being confined to the periphery of the polygon. It is possible to use nested polygons in the same device but care must be used to

retain the field direction with respect to the current in the vacuum switch (i.e. to maintain a parallel field and current path).

**D. External Circuit Configurations**

There are three major techniques for increasing the interruption characteristics of vacuum switches: counterpulse, saturable reactor and vacuum interrupters. These elements can be combined into a hybrid configuration for further enhancement of capabilities.

The main advantage of counterpulse techniques is the "artificial" creation of a current zero or extension of an existing current zero condition within the switch. Hence, the use of a counterpulse circuit is particularly useful for interruption of DC currents. Figure 3-3 shows a typical counterpulse circuit. The power source is assumed to be a quasi-DC source (e.g. a homopolar generator). The capacitor across the switch is charged in a negative sense so that when discharged it supplies a negative contribution to the current through the switch. This negative current cancels the DC current through the switch. The capacitor characteristics are chosen based on the power source open circuit voltage, the current to be cancelled and the temporal interruption characteristics of the switch.

Note that the current in the remainder of the switch loop does not decrease until an appreciable recovery voltage appears across the switch. It is at this point that the current is transferred into the load. The inductor connected across the capacitor in Figure 3-3 is used to re-initialize the bank by conducting for one half cycle to obtain capacitor voltage reversal.

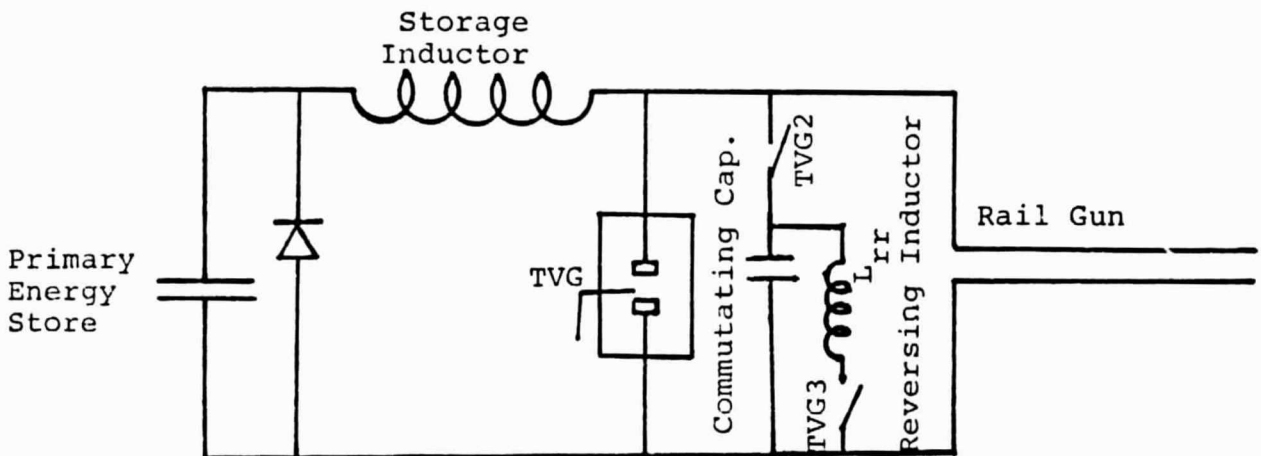


Figure 3-3 Counterpulse Circuit

Saturable reactors improve the interruption characteristics when used in series with the vacuum switch. Figure 3-4 shows a circuit with a saturable reactor element. The reactor is essentially a variable impedance device. The differential inductance is vastly different in a saturated reactor compared to an un-saturated reactor. The effect of coming out of saturation tends to prolong the time it takes the discharge to achieve a zero crossing. In other words the  $dI/dt$  during zero crossing can be reduced greatly as compared to the rest of the oscillating discharge. Thus, the gap plasma has a greater time to disperse and recover vacuum.

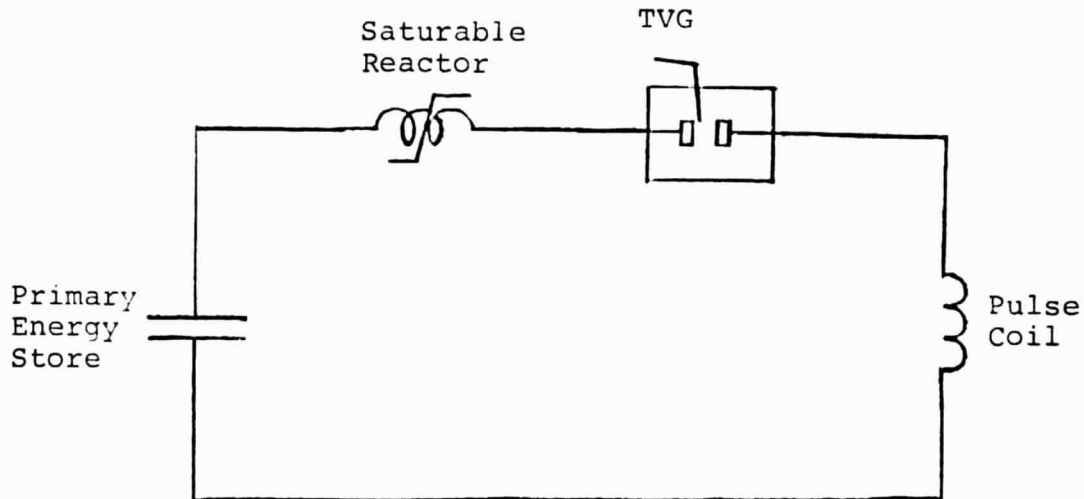


Figure 3-4 Saturable Reactor

Normally-closed circuits are readily achievable by use of vacuum interrupters or vacuum contacts. Solid metal-to-metal contact insures a small on-state resistance. Pressures of contact of 2500 psi are typical. A retracting motion of one of the contacts creates a vacuum arc by the vaporization and ionization of the last metal bridge of the separating contacts. Because of the mechanical motion involved, typical opening times of several milliseconds are common for these devices. Figure 3-5 shows a schematic of a vacuum interrupter circuit. When long discharge times are needed ( $> 10$  ms) some kind of contactor circuit is required to keep conduction losses manageable.

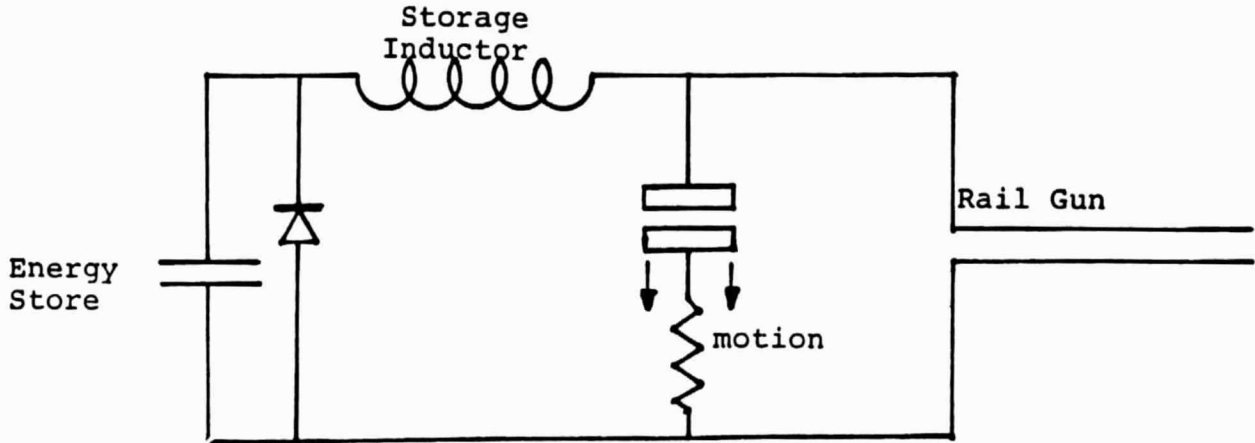


Figure 3-5 Vacuum Interrupter

Hybrid configurations combine the advantages of several techniques which increase the capabilities of vacuum switches. Figure 3-6 shows a possible hybrid circuit. A generalized power source is shown because the circuit characteristics should be comparable for either AC or DC power supplies.

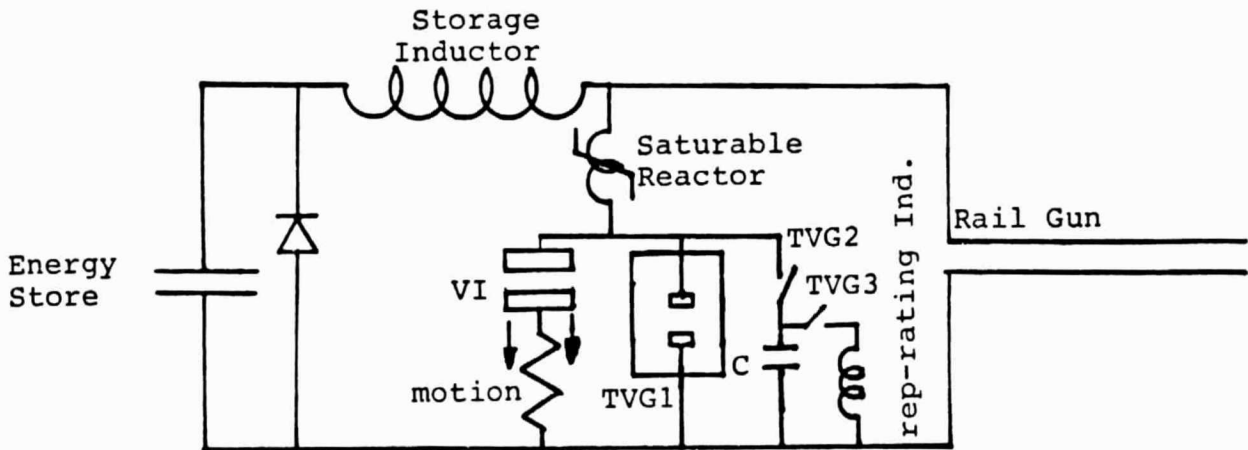


Figure 3-6 Hybrid Configurations

### E. Comparison with Competing Devices

Table 3-2 lists some indicative parameters of various switching devices. The values quoted are appropriate for a current pulse approximately 1 ms long.

Table 3-2 SINGLE SHOT RATINGS \*\*

<u>SWITCH</u>	<u>I<sub>max</sub></u>	<u>V<sub>max</sub></u>	<u>Charge/shot</u>	<u>Turn-on</u>	<u>Turn-off</u>
SCR	20 kA	2 kV	160C	1 $\mu$ s	5 $\mu$ s
Transistor	2 kA	800 V	20C	1 $\mu$ s	1 $\mu$ s
Vacuum Gap	80 kA	100 kV	100C	0.2 $\mu$ s	10 $\mu$ s
Gas Gap	100 kA	100 kV	100C	0.1 $\mu$ s	500 $\mu$ s
Thyratron	40 kA	40 kV	.001C	10 ns	1 $\mu$ s
Ignitron	600 kA	25 kV	1500C	0.5 $\mu$ s	10 ms

\*\* not simultaneous ratings

### F. Applications of Vacuum Switches

A simple EM launcher application of a vacuum switch is shown schematically in Figure 3-7. In this case an induction accelerator is controlled by a triggered vacuum switch. The LC frequency of the discharge is roughly 10 kHz. Alternative standard high current switches cannot combine the interruption and the high standoff voltage capability of the vacuum switch. The AC characteristic of the circuit shown in Figure 3-7 actually works to the advantage of the vacuum switch by providing current zeros for interruption. Furthermore, unused magnetic energy in the coil can be recovered by the capacitor and used again for subsequent shots. The inefficiencies in this process are then limited to only the ohmic losses incurred during the half-cycle discharge.

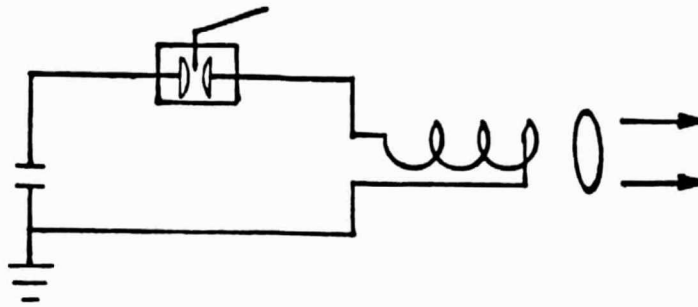


Figure 3-7 Inductive Vacuum Switch Schematic

The technique of energy recovery can be used in multi-stage devices as well. In general, a distributed energy system that requires separate energy stores for each stage does not permit energy recovery from one stage to the next. By interrupting the discharge at a naturally occurring current zero vacuum switch can recover unused energy at maximum efficiency. The same TVG can be used in a subsequent stage during the same shot to continue the acceleration.

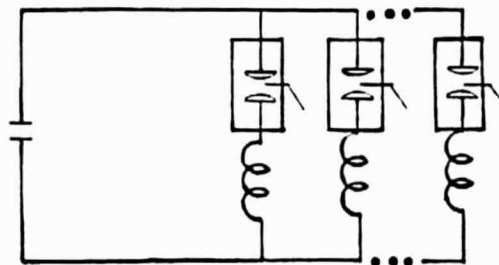


Figure 3-8 Multi-stage Induction Accelerator

Triggered vacuum gaps are also useful in rep-rated devices. Examples include: MPD thrusters and metallic induction reaction engines. [Mongeau, 1981] Vacuum switches permit the recovery of unused energy from one shot to the next, just like the recovery of energy from stage to stage in a distributed energy system. Typical operating parameters of such devices are shown in Figure 3-9.

Rep-rate	10-100 Hz
Peak current	10 kA
Induction frequency	10 kHz

Figure 3-9 Table of Typical Parameters of Reaction Engine

As discussed in Section 3 on arc conduction, there is a minimum voltage drop across the vacuum switch. This minimum voltage is a result of the electrode material choice and represents the energetic "overhead" which must be paid for vaporization and ionization of the cathode metal. Hence, it is energetically inefficient to have vacuum arc conduction in circumstances where the total circuit voltage is on the order of the arc drop. This is a particularly important issue in a low impedance device such as a railgun. The standard railgun circuit, for example, is shown in Figure 3-10.

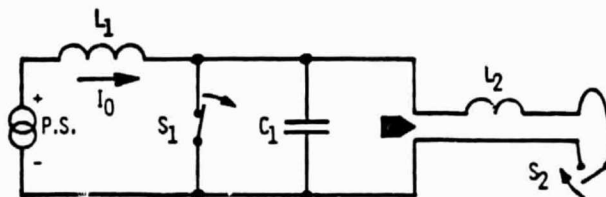


Fig. 8. Schematic diagram of an overpulse energy transfer and energy recovery circuit for a repetitive railgun system.

Figure 3-10 Railgun Schematic

The power source is typically a homopolar generator with an open circuit voltage of roughly 100 volts and a short circuit current capability of 1 MA. Due to the long charging times of the storage inductor ( $> 0.1$  second) a vacuum contactor must be used to reduce switch charging losses. The contactor can employ various hybrid techniques to produce a current zero in the switch for discharge purposes. The reader is referred to Honig for a more detailed account of vacuum gaps used in railgun circuits. The main advantage of using a hybrid vacuum switch is that very fast commutation ( $< 100$  usec) can be achieved. This is particularly important in very high velocity applications where the entire acceleration period can be less than a millisecond.

#### 4. Point Design

A point design has been developed for a high current rail gun. This design is based upon preceeding and present experimental work. Specifically, the circuit is designed to keep the electrode current density and the derivative of the current to be within present state of the art limitations.

Figure 4-1 shows the circuit under consideration. Table 4-1 lists the nominal device specifications. The circuit for the interrupting switch is complicated by the DC characteristic of rail gun operations. The basic operating scheme is: 1) the storage inductor is charged, 2) the current is commutated into the capacitor, 3) the projectile is injected into the rail gun, 4) the current is then tranferred from the capacitor branch of the circuit into the rail gun. The discharge can be rep-rated by re-triggering TVG-1 and repeating the procedure.

Solid metal-to-metal contacts are required for a low resistance and hence power loss during the storage inductor charging period. This contact is provided by a vacuum interrupter (VI). A triggered vacuum gap (TVG) in parallel with the VI will accept the transfer of current during the contact separation period. The VI and TVG-1 are conceptually different switches which may readily be combined into a single device to assure this current transfer.

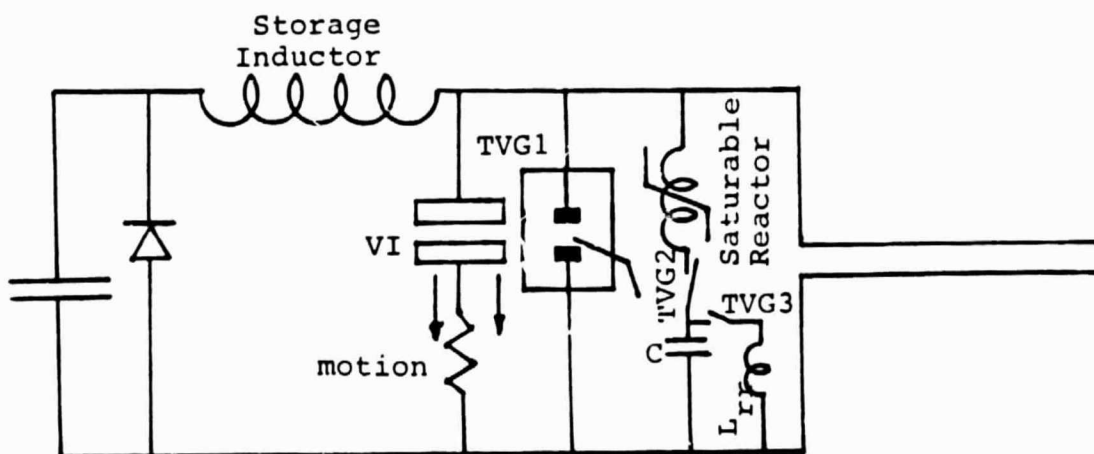


Figure 4-1 Point Design Circuit

Table 4-1 Point Design Parameters

Storage Coil

stored energy = 2.5 MJ  
 inductance = 5  $\mu$ H  
 current = 1 MA

Load

inductance = 1  $\mu$ H/m  
 transfer time = 50  $\mu$ s

Inductors

Saturable Reactor  
 inductance = 0.3  $\mu$ H - 1.3 mH

Rep. Rate Inductor  
 inductance = 3 mH

Capacitors

capacitance = 3.2 mf

Switches

ave. current  
 density = 200 A/cm<sup>2</sup>

VI

resistance = 1  $\mu$   
 contact force => 2500 kg<sub>2</sub>  
 contact area = 5000 cm<sup>2</sup>

TVG-1

max. current = 1 MA  
 electrode area = 5000 cm<sup>2</sup>  
 total charge = 1000 C  
 inter. time = 10  $\mu$ s

TVG-2

max. current = 1 MA  
 dI(I=0)/dt = 1000 A/ $\mu$ s

TVG-3

max. current = 10 kA  
 dI(I=0)/dt = 1 A/ $\mu$ s

A TVG is desirable as an additional circuit element due to the different demands required of the switches. The VI is designed to carry large currents with a very small switch resistance. The TVG-1 is designed to interrupt large currents very quickly. To date the use of vacuum interrupters in conjunction with capacitor counter-pulse circuits has been largely dedicated to 60 Hz power utility operation. Additional research at higher frequencies is needed to verify the feasibility of point design.

A capacitor counter-pulse is designed to provide a current zero within the TVG. The capacitor is pre-charged with the proper polarity to provide a current null at TVG-1. The capacitance is chosen based on the total charge needed to cancel the current in TVG-1, the desirable peak voltage, and the stored energy. The counterpulse is initiated by triggering another triggered vacuum gap TVG-2. The requirements for TVG-2 differ from those for TVG-1. Although the maximum current will be the same, TVG-1 must have a higher total charge transport (Coulomb) rating. Furthermore, because of the counterpulse, TVG-1 will have a low  $dI/dt$  interrupting rating because of the counterpulse. TVG-2, by contrast, must have a much higher  $dI/dt$  rating.

A saturable reactor is provided in series with TVG-2 to lower the current derivative. The saturated inductance is chosen by the peak current required and the chosen capacitance. The non-saturated inductance is chosen by the allowable current derivative at current zero.

An auxiliary inductor is switched by TVG-3 after TVG-2 commutates. This inductor is required to restore the polarity on the capacitor for subsequent discharges. The requirement for the inductor is to reverse the capacitor voltage within the allotted time during the load discharge. Typically, a rather large inductor may be chosen to reduce the peak current and the current derivative at current zero. Thus, TVG-3 has to meet minimal performance parameters.

It should be noted that devices illustrated as a single device could actually be several parallel devices due to help distribute and reduce peak switching loads per device.

## 5. Recommendations and Conclusions

Practical development of vacuum switches required solutions to various materials problems. Maintenance of a high degree of vacuum over the life of the device was not possible until the permanently sealed switch was developed. Ceramic-to-metal seals proved to be a critical issue.

Gas-free electrodes represented another basic advancement. Processes such as re-melting under a vacuum ambient release trapped gases which impair the interruption capability of the switch. Development of non-welding electrode contacts was another important advance.

It is likely that further developments in vacuum switch technology will occur in two specific areas. Materials will continue to provide significant advances for vacuum switches. In particular, electrode metallurgy and dielectric containment surfaces will benefit from research. Development of advanced electrical circuits will lead to new applications for these switches and effectively increase the overall characteristics of present-day switches.

Table 5-1 presents recommendations for continued vacuum switch research.

Table 5-1 Recommendations for Future Research

- \* Scaling Demonstration (currents approaching 1 MA)
- \* Materials Development
  - electrode issues: welding prevention  
low arc voltage desirable  
low erosion desirable
  - dielectric materials for vessel
- \* Innovative Geometries (similar to the rod array)
- \* Circuit Development
  - DC interruption tests
  - applied magnetic field for enhanced interruption performance

In conclusion, vacuum switches represent one of the best types of commutating switches in terms of peak currents and interruption time. Switching times of 1-2  $\mu$ s are common. Failure modes due to excessive currents are not catastrophic and

eventually recovery is assured. Lifetime of these devices is routinely in the tens of thousands of shots. Shelf life is approximately 20 years. Ideally adapted to space environments, these devices are impervious to high radiation and are orientation independent. They are generally much smaller than a gas gap switch of comparable interruption characteristics.

Operationally the triggered vacuum arc switch is very similar to a silicon controlled rectifier. The major disadvantage of vacuum switches is the rather large voltage drop associated with the arc conduction phase (about 50 volts).

The total energy dissipated in the switch should be a small fraction of the energy delivered to the load. Thus, vacuum switches are more naturally suited to high voltage and high impedance circuits. However, vacuum contactors are well suited for high current low voltage operation. The most exciting vacuum switch device is the so-called hybrid which combines a triggered gap with the conventional contactor. This device promises to be of great utility throughout the complete range of high power switching.

## 6. Appendix

### Experimental Research: Rationale and Results

Previous experiments have indicated a particularly promising approach to the design of vacuum switches. Interdigitated rod array structures offer advantages such as a parallel magnetic field and current path, relatively low "view factor" from rod to rod (similar to radiation heat transfer problems), and relatively high electrode surface area to volume ratio.

In 1980-81 General Electric pioneered experiments with this particular geometry. Their results showed great promise for a switch in the megampere range of currents. Unfortunately due to a variety of circumstances, they apparently did not follow-up on this device.

We have performed experiments on a modified version of the original General Electric design. Our main goals were to corroborate their results with this type of device and to establish some useful scaling relationships for higher current switches.

The switch consisted of two 2 rod electrode structures (see figure 6-1). The rods themselves were slightly tapered (about 5 degrees cone angle) and were made from a vacuum remelted maraging steel (Trade name VASCO MAX C-250; nominal analysis: 18.5 % Ni, &.5 % Co, 4.8 % Mo, 0.4 % Ti, 0.1 % Al, balance Fe). A separate trigger assembly was mounted in the center axis of the coaxial structure. The entire switch was housed in an 18 inch Pyrex glass cylinder used in previous vacuum gap work ( see Cope thesis).

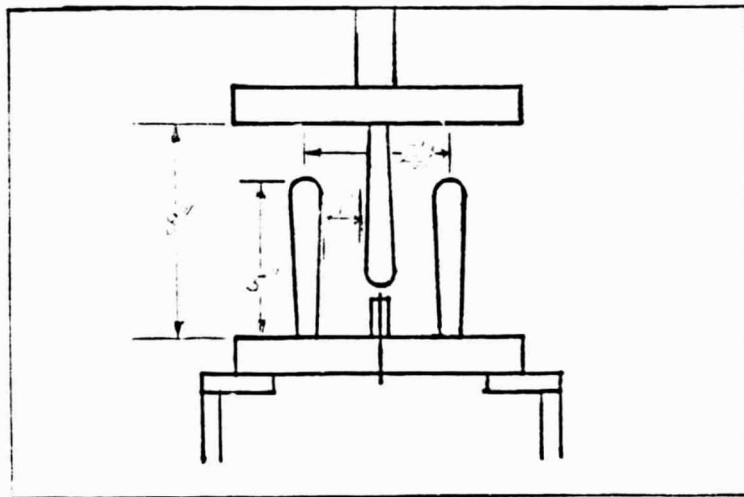


Figure 6-1 EML Rod Array Triggered Vacuum Gap Switch

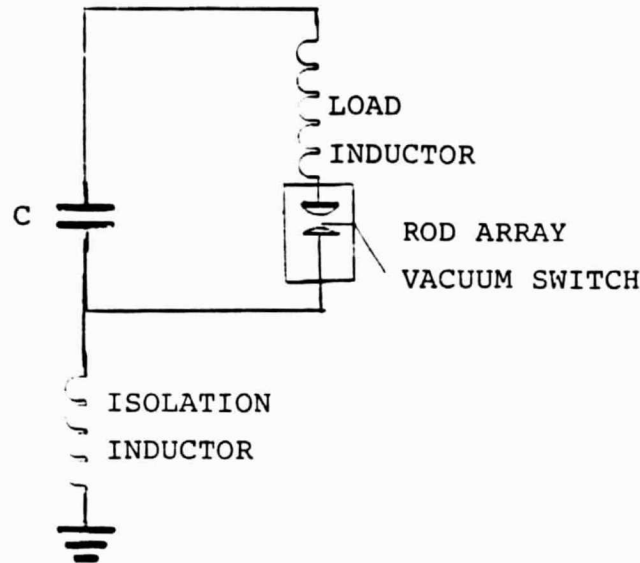


Figure 6-2 Experimental Circuit Diagram

The results of these experiments are summarized in Table 6-1. External circuit parameters were adjusted to give an oscillation frequency of from 1 kHz to 13 kHz. It was observed that the frequency multiplied by the peak current which was subsequently interrupted was approximately a constant.

Table 6-1 Experimental History of Rod Array Device

<u>Shot</u>	<u>Ind(uH)</u>	<u>Cap(uf)</u>	<u>Freq(kHz)</u>	<u>Volts(V)</u>	<u>Current(kA)</u>	<u>Idot(A/us)</u>
32	38	37.5	4.2	5	1	19
35	38	37.5	4.2	10	2	38
45	69	300	1.1	3	5	43
46	69	300	1.1	4	6.8	57
50	69	300	1.1	5	8.5	
52	69	300	1.1	7	12	80

[Note: device is scaled down for ease of experimentation.]

Intuitively, a higher frequency discharge allows less time for the plasma particles to vacate the interelectrode region. Boxman [Boxman, 1974] has shown that the plasma density increases proportionally to the current. If it is assumed that the density

decays approximately linearly with time following a current zero, and, if the time for decay is indicative of the frequency of the discharge, then it immediately follows that the product of frequency times peak current is independent of the frequency or the current.

The above observation implies that the peak  $dI/dt = wI$  is a function of switch geometry (electrode geometry and the proximity of dielectric surfaces) and of the materials used in the vacuum switch, and not a function of the actual circuit parameters.

The numerical results attained are as follows: a peak current of 22 kA was interrupted at a voltage of -6.2 kV. The discharge period was 943  $\mu s$  and the derivative with respect to time of the current was measured to be  $dI/dt = 150 A/\mu s$ . The average current density at the electrodes was approximately 180 A/cm<sup>2</sup>. The  $dI/dt$  interrupting rating appeared to be roughly independent of the discharge frequency.

The overall characteristics of our 4 rod device are compared with the GE device in Table 6-2.

Table 6-2 ROD ARRAY TRIGGERED VACUUM GAPS

	ESTABLISHED PERFORMANCE		EXTRAPOLATED PERFORMANCE
	EML SWITCH	GE SWITCH	
Application:	launchers	utilities	
I (KA)	22	100	50
dI/dt (A/ $\mu$ S)	150	30	3000
V (KV)	7	80	20
dV/dt (V/ $\mu$ S)	500	900	2000
frequency (Hz)	1000	60	10000
Tint ( $\mu$ s)	10	150	10

**REFERENCES**

- Boxman, R. L. 1974. J. Appl. Phys., 45, p. 4835.
- Cope, D. 1983. Metal Vapor Vacuum Arc Switching, Ph. D. dissertation, M. I. T. Physics Dept.
- Cope, D., Mongeau, P., Proc. Fourth IEEE Int'l Pulsed Power Conf., Albuquerque, N.M., 1983.
- Farrall, G. A. 1980. Vacuum Arcs: Theory and Applications ed. Lafferty (New York: Wiley), p. 228.
- Grissolm, J. T. and Newton, J. C. 1974. J. Appl. Phys. 45, p. 2885.
- Heberlein, J. V. R. and Gorman, J.G. 1980. IEEE Trans. on Plasma Science, PS-8, p. 283
- Honig, M., Proc. Fourth IEEE Pulsed Power Conf., Albuquerque, N.M., 1983.
- Honig, M., 1983. IEEE Trans. on Mag., MAG-20, pg. 312.
- Jenkins, J.E., et al, Jour. of Physics D, no. 8,1975, pg. L139.
- Kimblin, C. W. 1973. J. Appl. Phys., 44 p. 3074.
- Lafferty, J. M. 1966. Proc. IEER 54, p. 23.
- Mitchell, G. R. 1970. Proc. IEE 117, p. 2315.
- Mongeau, P., 1982, Coaxial Air-Core Electromagnetic Accelerators Ph. D. thesis, MIT Physics.
- Nunnally, W. C., Proc Fourth IEEE Pulsed Power Conf, Albuquerque, N.M., 1983, pg. 620.
- O'Hanlon, J. F. 1980. A User's Guide to Vacuum Technology (ew York: Wiley).
- Plyutto, A. A., Ryzhkov, V. N. and Kapin, A. T. 1965. Sov. Phys. JETP 20, p. 328.
- Rondeel, W., J. Physics D, no. 6, 1973, pg. 1705.
- Sze, A., Goldman, E. and Brooks, IEEE Transactions on Magnetics, vol. 20, no. 2, March 1984, pg 308.
- Tuma, D.T., et al, J. Appl. Phys., no. 49, 1978, pg. 3821.